

REVIEW ARTICLE

Cerebral malaria in children: using the retina to study the brain

Ian J. C. McCormick,^{1,2} Nicholas A. V. Beare,^{2,3} Terrie E. Taylor,^{5,6} Valentina Barrera,² Valerie A. White,⁷ Paul Hiscott,² Malcolm E. Molyneux,^{1,4,8} Baljean Dhillon^{9,10} and Simon P. Harding^{2,3}

1 Malawi-Liverpool-Wellcome Trust Clinical Research Programme, PO Box 30096, Chichiri, Blantyre 3, Malawi

2 University of Liverpool, Department of Eye and Vision Science, Faculty of Health & Life Sciences, University of Liverpool Room 356, 4th Floor, UCD Building, Daulby Street, Liverpool L69 3GA, UK

3 Royal Liverpool University Hospital, St. Paul's Eye Unit, Prescot St, Liverpool, Merseyside L7 8XP, UK

4 University of Malawi College of Medicine, College of Medicine, P/Bag 360 Chichiri, Blantyre 3 Malawi

5 Blantyre Malaria Project, Blantyre, Malawi

6 Michigan State University, Department of Osteopathic Medical Specialities, West Fee Hall, 909 Fee Road, Room B305, East Lansing, MI 48824, USA

7 Vancouver General Hospital, Department of Pathology and Laboratory Medicine, Vancouver, B.C. V5Z1M9, Canada

8 Liverpool School of Tropical Medicine, Liverpool School of Tropical Medicine, Pembroke Place, Liverpool, L3 5QA, UK

9 University of Edinburgh, Department of Ophthalmology, Edinburgh, UK

10 Princess Alexandra Eye Pavilion, Edinburgh, UK

Correspondence to: Ian J.C. McCormick,
Malawi-Liverpool-Wellcome Trust Clinical Research Programme,
PO Box 30096, Chichiri,
Blantyre 3, Malawi
E-mail: ian.mccormick@gmail.com

Cerebral malaria is a dangerous complication of *Plasmodium falciparum* infection, which takes a devastating toll on children in sub-Saharan Africa. Although autopsy studies have improved understanding of cerebral malaria pathology in fatal cases, information about *in vivo* neurovascular pathogenesis is scarce because brain tissue is inaccessible in life. Surrogate markers may provide insight into pathogenesis and thereby facilitate clinical studies with the ultimate aim of improving the treatment and prognosis of cerebral malaria. The retina is an attractive source of potential surrogate markers for paediatric cerebral malaria because, in this condition, the retina seems to sustain microvascular damage similar to that of the brain. In paediatric cerebral malaria a combination of retinal signs correlates, in fatal cases, with the severity of brain pathology, and has diagnostic and prognostic significance. Unlike the brain, the retina is accessible to high-resolution, non-invasive imaging. We aimed to determine the extent to which paediatric malarial retinopathy reflects cerebrovascular damage by reviewing the literature to compare retinal and cerebral manifestations of retinopathy-positive paediatric cerebral malaria. We then compared retina and brain in terms of anatomical and physiological features that could help to account for similarities and differences in vascular pathology. These comparisons address the question of whether it is biologically plausible to draw conclusions about unseen cerebral vascular pathogenesis from the visible retinal vasculature in retinopathy-positive paediatric cerebral malaria. Our work addresses an important cause of death and neurodisability in sub-Saharan Africa. We critically appraise evidence for associations between retina and brain neurovasculature in health and disease, and in the process we develop new hypotheses about why these vascular beds are susceptible to sequestration of parasitized erythrocytes.

Keywords: cerebral malaria; cerebral microvasculature; retinal microvasculature; haemorheology; surrogate marker

Received May 27, 2013. Revised October 16, 2013. Accepted November 17, 2013. Advance Access publication February 26, 2014

© The Author (2014). Published by Oxford University Press on behalf of the Guarantors of Brain.

This is an Open Access article distributed under the terms of the Creative Commons Attribution License (<http://creativecommons.org/licenses/by/3.0/>), which permits unrestricted reuse, distribution, and reproduction in any medium, provided the original work is properly cited.

Abbreviation: CI = confidence interval; CM = cerebral malaria; CMRgluc = cerebral metabolic rate (glucose); CMRO2 = cerebral metabolic rate (oxygen); CNP = capillary non-perfusion; CRAE = central retinal artery equivalent; CRVE = central retinal vein equivalent; DD = disc diameter; FA = fluorescein angiogram; FAZ = foveal avascular zone; ICAM-1 = intercellular adhesion molecule 1; LDR = length to diameter ratio; MRI = magnetic resonance imaging; OR = odds ratio; PfEMP-1 = *Plasmodium falciparum* erythrocyte membrane protein 1; SD = standard deviation

Introduction

Paediatric cerebral malaria is a clinical syndrome that kills and disables children through mechanisms that remain incompletely understood. Adhesion of parasitized erythrocytes to the microvascular endothelium, leading to their sequestration in the brain, is the pathological signature of both adult and paediatric cerebral malaria, and is thought to be the chief cause of injury (Taylor *et al.*, 2004; Ponsford *et al.*, 2012). Several hypothetical mechanisms linking sequestration, which is entirely intravascular, to extravascular parenchymal damage have been proposed (Van der Heyde *et al.*, 2006) but questions remain about which of these mechanisms are most important, how they might interact, and ultimately where new therapies should be directed. One of the reasons why such questions remain over 100 years after sequestration was first identified is because *in vivo* access to the brain is difficult, and advances in knowledge have relied on post-mortem and *in vitro* studies. Improved understanding of *in vivo* neurovascular pathogenesis and the development of better treatments will be facilitated by disease models or surrogate markers.

The retina may be a good source of surrogate markers of cerebrovascular injury because paediatric cerebral malaria is associated with a retinopathy ('malarial retinopathy') that accurately predicts cerebral sequestration (Taylor *et al.*, 2004), correlates with severity of brain involvement (White *et al.*, 2001), and is associated with mortality (Beare *et al.*, 2004). Unlike the brain, the eye allows non-invasive access for structural and functional imaging of the microcirculation, which is thought to be the major site of sequestration.

The concept that neurovascular injury observed in the retina resembles neurovascular injury lying unseen in the brain is based on the assumption that the two circulations are analogous in ways that are relevant to the pathogenesis of paediatric cerebral malaria. Such assumptions should be supported by a biologically plausible rationale before specific retinal vascular features are considered as surrogate markers of cerebrovascular damage (International Conference on Harmonisation, 1998).

Is such a rationale likely? It is well known that the retina and brain have many similarities. Both are part of the CNS, with common embryological origins, vascular structure and metabolic demands. The relevance of these similarities for potential surrogate markers has been recognized (Patton *et al.*, 2005, 2006), especially for stroke (Doubal *et al.*, 2009, 2010). Despite this, detailed comparisons of the microvasculature of the two organs are rare (Cogan and Kuwabara, 1984; Patton *et al.*, 2005).

Our objective was to discover how likely it is that the retinal vascular damage responsible for malarial retinopathy reflects analogous cerebrovascular damage in retinopathy-positive paediatric cerebral malaria. To do this we compared the manifestations

of paediatric cerebral malaria in retina and brain, and then compared retina and brain in terms of vascular features likely to be important for cerebral malaria pathogenesis. Concluding that retina and brain are analogous in ways relevant to this disease would justify further investigation to see whether specific retinal signs predict both focal brain damage detectable by MRI and the patient's response to treatment. The results of such investigations would address further criteria of surrogacy (International Conference on Harmonisation, 1998), and in the context of a strong biological rationale could shed light on the dynamics of cerebral malaria neurovascular pathogenesis in the period between coma onset and recovery or death.

Malarial retinopathy can occur in parasitaemic children without cerebral malaria (Beare *et al.*, 2004), and indeed, some features of malarial retinopathy occur in conditions that don't involve malaria at all (e.g. white-centred haemorrhages). It is not clear if retinopathy predicts cerebral sequestration in malarial syndromes besides paediatric cerebral malaria, or how often retinopathy might occur in severely ill children in general.

We therefore discuss retinopathy in the specific clinical context of paediatric cerebral malaria. In this particular population malarial retinopathy has high positive and negative predictive value to distinguish between the presence and absence of cerebral sequestration in fatal cases (Taylor *et al.*, 2004). Until associations between retinopathy and cerebral sequestration are known for malaria in general, extrapolation from our review to severe malaria syndromes other than paediatric cerebral malaria may not be appropriate.

Our review is divided into four sections. In the first section we describe paediatric cerebral malaria, including the typical clinical presentation, manifestations of cerebral malaria in the brain, and manifestations in the retina. The neurovascular effects of cerebral malaria on retina and brain are then compared.

In the second section we introduce the concept that patterns of neurovascular pathology in retina and brain may be understood in terms of haemorrhological dysfunction involving microvascular haematocrit, blood viscosity and shear stress. These factors depend on interactions between intrinsic properties of blood and structural properties of microvascular networks, and this suggests that microvascular architecture may be a useful point of comparison for a cerebral malaria-specific analogy between retina and brain.

The third section describes microvascular architecture in the human retina and brain, and compares features that may be relevant to the pathogenesis of cerebral malaria.

We end by discussing how our comparison of retina and brain provides a biologically plausible rationale for considering retinal signs as potential surrogates of brain damage in retinopathy-positive paediatric cerebral malaria. We consider how observations of retinal vessel structure and function might allow inference of *in vivo* cerebrovascular pathogenesis.

Paediatric cerebral malaria

Definition

Several species of *Plasmodium* parasite cause malaria in humans. *P. falciparum* is responsible for the majority of severe malaria and malaria-associated deaths worldwide, particularly in sub-Saharan Africa where severe malaria has a disproportionate impact on children <5 years of age (WHO, 2012). In children, severe malaria predominantly involves one or more of three syndromes: cerebral malaria, severe malarial anaemia and metabolic acidosis. Other manifestations of paediatric severe malaria include convulsions, hypoglycaemia, hyperparasitaemia and prostration (WHO, 2000). Cerebral malaria is defined as coma, with *P. falciparum* peripheral parasitaemia, in the absence of another identifiable cause of coma, such as hypoglycaemia or meningitis (Newton *et al.*, 1998). This definition is broad, and misclassifies almost 25% of fatal paediatric cases as cerebral malaria when compared with histopathological identification of sequestration in cerebral vessels as the reference standard. The presence of malarial retinopathy on pre-mortem fundus examination accurately distinguishes histopathological cerebral malaria from cases that meet the clinical definition but actually have another cause of death (Taylor *et al.*, 2004). Although the strong association between retinopathy and intracerebral sequestration has been established only in fatal cases, it is likely that the association also prevails in those who recover, and that the presence of retinopathy improves the accuracy of diagnosis in children with cerebral malaria (Beare *et al.*, 2011).

Typical presentation and clinical course

In an area with intense transmission of *P. falciparum*, the typical history of paediatric cerebral malaria involves a young child who rapidly develops coma after a short prodrome of fever and generalized illness. The coma may be preceded or accompanied by convulsions, from which the child does not wake. On examination the child is usually febrile, and may have deep or rapid breathing. Coma is distinguished from prolonged post-ictal state by duration >30 min after seizure. Depth of coma is assessed using a modification of the Glasgow Coma Scale, known as the Blantyre Coma Scale (Molyneux *et al.*, 1989; WHO, 2000, 2010). Convulsions or posturing, including opisthotonus, may be present. Ophthalmoscopy through dilated pupils reveals signs of malarial retinopathy: white patchy discolouration of the macula and/or peripheral retina; orange or white discolouration of retinal vessels; and/or retinal haemorrhages, typically with white centres. Papilloedema may be seen, but in isolation does not distinguish cerebral malaria from other causes of coma (Lewallen *et al.*, 1999, 2008; Harding *et al.*, 2006). Investigation may reveal concomitant metabolic acidosis and/or severe anaemia. Peripheral *P. falciparum* asexual parasitaemia is present by definition. Other treatable causes of coma in this setting must be ruled out and include malaria-associated hypoglycaemia and meningitis. Bacteraemia may be found, especially in infants and in the presence of severe anaemia (Bronzan *et al.*, 2007).

The duration of illness is usually short, and most patients recover or die within 48 h. Death is typically by respiratory arrest, and case fatality with treatment is ~15%. Those who recover are at risk of neurodisability (Molyneux *et al.*, 1989) and epilepsy (Birbeck *et al.*, 2010). Guidelines for treatment have been published (WHO, 2010).

Cerebral malaria also occurs in adults (Table 1). The clinical presentation is different from paediatric cerebral malaria (WHO, 2000), but it is not clear if this is because of age or differences in immunology related to transmission intensity (Idro *et al.*, 2005). The geographical distribution is different from that of paediatric cerebral malaria. Adult cerebral malaria occurs primarily in South and South East Asia, where transmission of *P. falciparum* is endemic and seasonal and most children and adults have no immunity; whereas paediatric cerebral malaria occurs mainly in sub-Saharan Africa where transmission is endemic and where both older children and adults have acquired partial immunity. Adult travellers who are *P. falciparum* naïve may develop cerebral malaria in endemic countries. Patterns of mortality and comorbidity vary with age (Dondorp *et al.*, 2008).

Malarial retinopathy has been described in adults since at least the 1800s (Mackenzie, 1877). Maude *et al.* (2009) found retinopathy in 14/20 (70%) adults with cerebral malaria, 17/20 (85%) with other types of severe malaria, and 9/15 (60%) with uncomplicated malaria. The retinopathy was most severe in those with cerebral malaria. Abu Sayeed *et al.* (2011) found retinopathy in 31/75 (41%) with cerebral malaria, 16/64 (25%) with other types of severe malaria, and 1/31 (3%) with uncomplicated malaria. Number of retinal haemorrhages was an independent predictor of death. Both studies used sensitive retinal imaging techniques and a standardized grading scheme (Harding *et al.*, 2006), but neither found the characteristic vessel discolouration seen in up to 30% of children with cerebral malaria (Beare *et al.*, 2004). Compared with the adult literature, few data exist on the presence of malarial retinopathy in children with uncomplicated malaria, as consistent retinal examination of conscious children is difficult—particularly so for the retinal periphery. Further research is needed.

Manifestations of retinopathy-positive cerebral malaria in the paediatric brain

Sequestration

Sequestration is the histopathological hallmark of paediatric cerebral malaria (Taylor *et al.*, 2004). Sequestration results from the binding of parasitized erythrocytes to vascular endothelium. Parasitized erythrocytes also bind *in vitro* to other erythrocytes (rosetting), and to platelets (clumping, or auto-agglutination). Sequestration is mediated by adhesion between malarial antigens on the surface of the infected erythrocyte and several host receptors on the vascular endothelium. The *P. falciparum* surface antigen most studied is *P. falciparum* erythrocyte membrane protein 1

Table 1 Manifestations of cerebral malaria in the retina and brain

	Paediatric retina	Paediatric brain	Adult brain
Sequestration	Always present in fatal cerebral malaria (Lewallen <i>et al.</i> , 2000). Unclear if absent in fatal coma of other cause or severe malarial anaemia.	Always present in fatal cerebral malaria, and absent in fatal coma of other cause (Taylor <i>et al.</i> , 2004; Dorovini-Zis <i>et al.</i> , 2011). Commonly associated with sequestered leucocytes (Brown <i>et al.</i> , 2001; Armah <i>et al.</i> , 2005)	Always present in fatal cerebral malaria (MacPherson <i>et al.</i> , 1985; Oo <i>et al.</i> , 1987; Pongponratn <i>et al.</i> , 1991; Sein <i>et al.</i> , 1993). In cerebral malaria density is greater in brain than other organs (MacPherson <i>et al.</i> , 1985; Pongponratn <i>et al.</i> , 1991). Significant sequestration may be present in fatal non-cerebral malaria (MacPherson <i>et al.</i> , 1985; Silamut <i>et al.</i> , 1999). The percentage of vessels with sequestration is greater in cerebral malaria than non-cerebral malaria (Ponsford <i>et al.</i> , 2012)
Frequency			
Location	Patchy distribution within capillary network (Lewallen <i>et al.</i> , 2000). Variation between retinal regions not yet defined.	Most microvessels, and the margins of pial and larger vessels (Dorovini-Zis <i>et al.</i> , 2011). Grey and white matter of cerebrum, subcortex, brainstem and cerebellum (Armah <i>et al.</i> , 2005; Dorovini-Zis <i>et al.</i> , 2011).	Occurs in capillaries, venules, and very occasional arterioles (MacPherson <i>et al.</i> , 1985). Occurs in grey and white matter, but most dense in cerebral white matter (Nagatake <i>et al.</i> , 1992). Density reduces from cerebrum to cerebellum to brainstem (Pongponratn <i>et al.</i> , 2003). Density greater in cerebellum than cerebrum (Sein <i>et al.</i> , 1993).
Vessels involved	Capillaries and margins of larger vessels (Lewallen <i>et al.</i> , 2000). Vessel discolouration affects capillaries, venules, and arterioles (personal observation)	Occurs in brain microvessels, pial and larger vessels (Dorovini-Zis <i>et al.</i> , 2011)	Predominant site is the capillary bed, but also occurs in larger pial and subarachnoid vessels (Spitz, 1946). Uncommon in arterioles (MacPherson <i>et al.</i> , 1985).
Haemorrhages	Type White-centred, blot (White <i>et al.</i> , 2001). Parasitized erythrocytes rarely seen outside vessel (White <i>et al.</i> , 2001).	Ring (Dorovini-Zis <i>et al.</i> , 2011). Parasitized erythrocytes rarely seen outside vessel (White <i>et al.</i> , 2001; Dorovini-Zis <i>et al.</i> , 2011).	Ring, perivascular (Spitz, 1946; Nagatake <i>et al.</i> , 1992; Sein <i>et al.</i> , 1993; Turner, 1997). Parasitized erythrocytes are seen outside vessel (Sein <i>et al.</i> , 1993; Turner, 1997).
Frequency	Gross haemorrhages present in 78% fatal cerebral malaria, 7% fatal coma of other cause (White <i>et al.</i> , 2009).	Any type present in 80% fatal cerebral malaria (Dorovini-Zis <i>et al.</i> , 2011).	Ring haemorrhages present in up to 30% of cases of fatal cerebral malaria (Spitz, 1946). No significant difference in haemorrhage frequency between cerebral malaria (~60% of cases) and non-cerebral malaria (~40% of cases) (Medana <i>et al.</i> , 2011).
Location	All retinal quadrants. Usually restricted to inner retinal layers, with extension to subretinal haemorrhage in severe cases (White <i>et al.</i> , 2009).	Common in white matter, rare in grey matter except in the cerebellum (White <i>et al.</i> , 2001; Dorovini-Zis <i>et al.</i> , 2011).	Usually occur in cerebral white matter; also reported in pons, medulla, cerebellum, and cortical grey matter (Spitz, 1946; Nagatake <i>et al.</i> , 1992; Sein <i>et al.</i> , 1993; Turner, 1997). No difference in haemorrhage frequency between cortex, diencephalon, and brainstem (Medana <i>et al.</i> , 2011).
Vessel leakage	Type Fibrinogen leakage along vessels with and without associated haemorrhage (White <i>et al.</i> , 2009).	Fibrinogen leakage often associated with haemorrhage, can be independent of haemorrhage (Dorovini-Zis <i>et al.</i> , 2011).	Rarefaction of the perivascular space, perivascular pools of proteinaceous material, vacuolar parenchymal oedema, oedema between fibres of white matter tracts, fluid-filled spaces between myelin fibres. No difference between fatal cerebral and non-cerebral malaria (Medana <i>et al.</i> , 2011).

(continued)

Table 1 Continued

	Paediatric retina	Paediatric brain	Adult brain
Frequency	Fibrinogen leakage in 31 % cases fatal cerebral malaria, 7% fatal coma of other cause (White <i>et al.</i> , 2009). Average (SD) number of foci is 1.2 (2.6) in fatal cerebral malaria and 0.21 (1.1) in coma of other cause (White <i>et al.</i> , 2009).	Unclear how many cases of fatal cerebral malaria have leakage of any type. Leakage greater in white than grey matter (associated with haemorrhages) (Dorovini-Zis <i>et al.</i> , 2011). Cerebral white and grey matter, subcortex, brainstem and cerebellum (Dorovini-Zis <i>et al.</i> , 2011).	At least one type of oedema present in all cases of both cerebral and non-cerebral malaria (Medana <i>et al.</i> , 2011). Oedema between white matter tract fibres is most common in: brainstem > diencephalon > cortex (Medana <i>et al.</i> , 2011). Brainstem, diencephalon, cerebral cortex (Medana <i>et al.</i> , 2011).
Location/vessels involved	Associated with vessels but not defined in terms of retinal quadrants or vessel type (White <i>et al.</i> , 2009). Angiographic fluorescein leakage predominantly affects venules (Beare <i>et al.</i> , 2009). Retinal whitening and capillary non-perfusion appears to be especially prominent at the foveal avascular zone, horizontal raphe, and retinal periphery. All are watershed regions (Beare <i>et al.</i> , 2009).	Regions where MRI brain signal changes distinguish between retinopathy-positive and negative cerebral malaria (highest to lowest odds ratio): basal ganglia, corpus callosum, cerebral cortex, thalamus, cerebral white matter, posterior fossa (Potchen <i>et al.</i> , 2012).	Regions reported to be involved: Brain stem, thalamus, cerebellum, corpus callosum, cerebral white matter (Yadav <i>et al.</i> , 2008; Rasalkar <i>et al.</i> , 2011).
Regions vulnerable to presumed ischaemia on imaging			

(PfEMP1), which is encoded by a family of *var* genes (reviewed in Craig and Scherf, 2001; Rowe *et al.*, 2009; Miller *et al.*, 2013). PfEMP1 undergoes antigenic variation, associated with differential sequestration between organs in children (Montgomery *et al.*, 2007). Of several host receptors, intercellular adhesion molecule 1 (ICAM1) has received most attention. ICAM1 is a cytokine-inducible endothelial receptor normally involved in leucocyte rolling before firm endothelial adhesion, and is upregulated in brain vessels in fatal paediatric cerebral malaria (Brown *et al.*, 2001; Armah *et al.*, 2005). Because sequestration results from adhesion between antigens and receptors, it is likely to be influenced by shear stress (Kaul *et al.*, 1991; Fedosov *et al.*, 2011a, b).

In fatal paediatric cerebral malaria, sequestration is seen in most microvessels of both grey and white matter of the cerebral hemispheres. Sequestration occurs on the margins of larger pial and subarachnoid vessels (Dorovini-Zis *et al.*, 2011), but a calibre threshold above which sequestration does not occur has not been described. Sequestration is thought to be most severe in capillaries and postcapillary venules—although only one study, in adults, has compared sequestration between vessel types (MacPherson *et al.*, 1985).

Sequestration seems to be a fundamental component of cerebral malaria pathogenesis, but exact mechanisms linking it to tissue injury in cerebral malaria are unclear. Microvascular obstruction from sequestration leads to impaired perfusion, but also endothelial activation associated with apoptosis, reduced dilatatory capacity, and a procoagulant state (Moxon *et al.*, 2009; Rowe *et al.*, 2009). Parasitized erythrocytes bind to endothelial protein C receptor (Turner *et al.*, 2013). The associated loss of protein C receptor in cerebral vessels is likely to result in unmodified signalling through several molecular cascades leading to inflammation, loss of vascular barrier function, activation of platelets and production of fibrin (Moxon *et al.*, 2013).

Endothelial dysfunction may also result from *P. falciparum*-associated reductions in nitric oxide (NO) synthesis and bioavailability (reviewed in Miller *et al.*, 2013), and increased oxidative stress (Griffiths *et al.*, 2001; Narsaria *et al.*, 2012), which can reduce erythrocyte deformability (Dondorp *et al.*, 1997, 2003) and impair neurovascular coupling as well as control of vascular tone (reviewed in Faraci, 2011).

These points illustrate how tissue damage associated with sequestration may be caused through synergistic mechanisms, including (and probably not limited to) inflammation and coagulation, in addition to congestion of blood flow secondary to reductions in lumen diameter. Local coagulopathy and loss of endothelial barrier function are consistent with haemorrhage and brain swelling seen in the paediatric brain, and with quantifiable manifestations of malarial retinopathy.

Haemorrhage

Histopathology reveals subtypes of cerebral malaria within fatal retinopathy-positive paediatric cerebral malaria. In Malawi 75% of cases coming to autopsy have sequestration with associated perivascular haemorrhages and intravascular microthrombi, whereas 25% have sequestration but no haemorrhages or other

perivascular pathology visible on routine haematoxylin and eosin-stained sections (Dorovini-Zis *et al.*, 2011).

Petechial haemorrhages on the cut surface of fresh brain correspond to microscopic ring haemorrhages. Ring haemorrhages occur frequently in the white matter of the cerebral hemispheres, and extend to the grey–white border. They are rare in cortical and subcortical grey matter, but occur throughout the cerebellum and brainstem (White *et al.*, 2001). Diffuse axonal injury follows the same distribution (Dorovini-Zis *et al.*, 2011).

In general, ring haemorrhages in paediatric cerebral malaria consist of extravasated uninfected erythrocytes; each haemorrhage is centred on a distended capillary containing infected erythrocytes and commonly a microthrombus (Dorovini-Zis *et al.*, 2011).

Brain swelling and vessel leakage

Studies of paediatric cerebral malaria where retinopathy status was either unknown or a combination of retinopathy-positive and retinopathy-negative cases, have found raised opening pressure at lumbar puncture (Newton *et al.*, 1991), clinical signs consistent with brain herniation (12/12 fatal cases, 17/49 survivors) (Newton *et al.*, 1994), papilloedema (Beare *et al.*, 2004), and enlarged optic nerve sheath diameter (Beare *et al.*, 2012).

Raised brain weight and extravasation of fibrinogen from microvessels occurs in histopathologically confirmed paediatric cerebral malaria, although these do not distinguish cerebral malaria from fatal coma of other cause. Leakage is most often associated with vascular pathology such as haemorrhage, but fibrinogen is also seen in cerebral grey matter where haemorrhages are absent (Dorovini-Zis *et al.*, 2011). Focal loss of blood–brain barrier cell junction proteins (ZO1, occludin, vinculin) occurs adjacent to sequestration. The distribution of fibrinogen, IgG and C5b-9 in these cases did not indicate widespread leakage into brain tissue (Brown *et al.*, 2001).

Brain imaging

Consistent with reports of raised intracranial pressure in clinically defined paediatric cerebral malaria, MRI in retinopathy-positive paediatric cerebral malaria reveals moderate to severe brain swelling in 47% (57/120) of cases. This is significantly more common than in paediatric cerebral malaria without retinopathy [7/32 cases, OR 3.2, 95% CI 1.3–8] (Potchen *et al.*, 2012).

Discrete lesions are seen in basal ganglia, thalamus, corpus callosum, and cerebral grey and white matter. All are significantly more frequent in retinopathy-positive cerebral malaria than retinopathy-negative cases. Cortical abnormalities can be predominantly frontal or posterior. Lesions do not respect arterial watersheds (Potchen *et al.*, 2012), but may reflect territories of venous drainage (Meder *et al.*, 1994; Andeweg, 1996). Distribution of lesions according to venous territories is consistent with sequestration occurring primarily on the venous side of the microvasculature.

Manifestations of cerebral malaria in the paediatric retina

Several clinical (Harding *et al.*, 2006) and fluorescein angiographic features of malarial retinopathy (Beare *et al.*, 2009) are illustrated in Fig. 1. Standard images of all features are in Harding *et al.*, (2006).

Sequestration in retinal vessels

Sequestration is distributed unevenly in capillaries and the margins of larger retinal vessels (Lewallen *et al.*, 2000). Sequestration and vessel discoloration tend to occur at vascular branch points (Lewallen *et al.*, 2000), where greater turbulence exists to disrupt laminar flow (Nagaoka and Yoshida, 2006). It has been proposed that de-haemoglobinization of parasitized erythrocytes is responsible for the clinically observed white or orange discoloration of retinal vessels seen in paediatric cerebral malaria (Lewallen *et al.*, 2000). Retinal vessels, particularly venules, can have a mottled appearance on fluorescein angiogram, which may represent sequestration (Beare *et al.*, 2009). The discoloration and mottled appearance of retinal vessels in malarial retinopathy appears to be pathognomonic for paediatric severe malaria, but is reported in severe malarial anaemia as well as cerebral malaria (Beare *et al.*, 2004).

Retinal vessel leakage

Fluorescein leakage is seen in ~40% of cases with malarial retinopathy and indicates blood–retinal barrier disruption. It does not co-localize with vessel mottling (Beare *et al.*, 2009). White *et al.* (2009) reported leakage of fibrinogen from retinal vessels in 31% (11/35) of cases with cerebral malaria versus 7% (2/29) coma of other cause. Leakage was not reported in terms of vessel type, but fluorescein angiogram imaging suggests that leaking is predominantly from venules (Beare *et al.*, 2009) (Fig. 1). Again, this is consistent with cerebral malaria pathogenesis centring on capillaries and post-capillary venules.

Retinal whitening

Retinal whitening appears as discrete areas of pale discoloration of the retina (Fig. 1A), which correspond to areas of capillary non-perfusion seen on fluorescein angiogram. Retinal whitening and capillary non-perfusion seem to occur earliest and most severely in watershed regions such as the margin of the foveal avascular zone, horizontal raphe and retinal peripheries (Beare *et al.*, 2009). In contrast to the scattered geometric lesions seen in the macula, whitening and capillary non-perfusion in the retinal periphery can occur in large tide-mark distributions that cut across arterioles and venules of varying sizes (Beare *et al.*, 2009) (Fig. 1B).

Whitening is likely to be caused by oncotic cell swelling in response to reduced perfusion (Beare *et al.*, 2009). Other possible mechanisms include metabolic steal by large numbers of parasites (Hero *et al.*, 1997), and occlusion caused by microthrombi (White *et al.*, 2009). These theories are not mutually exclusive.

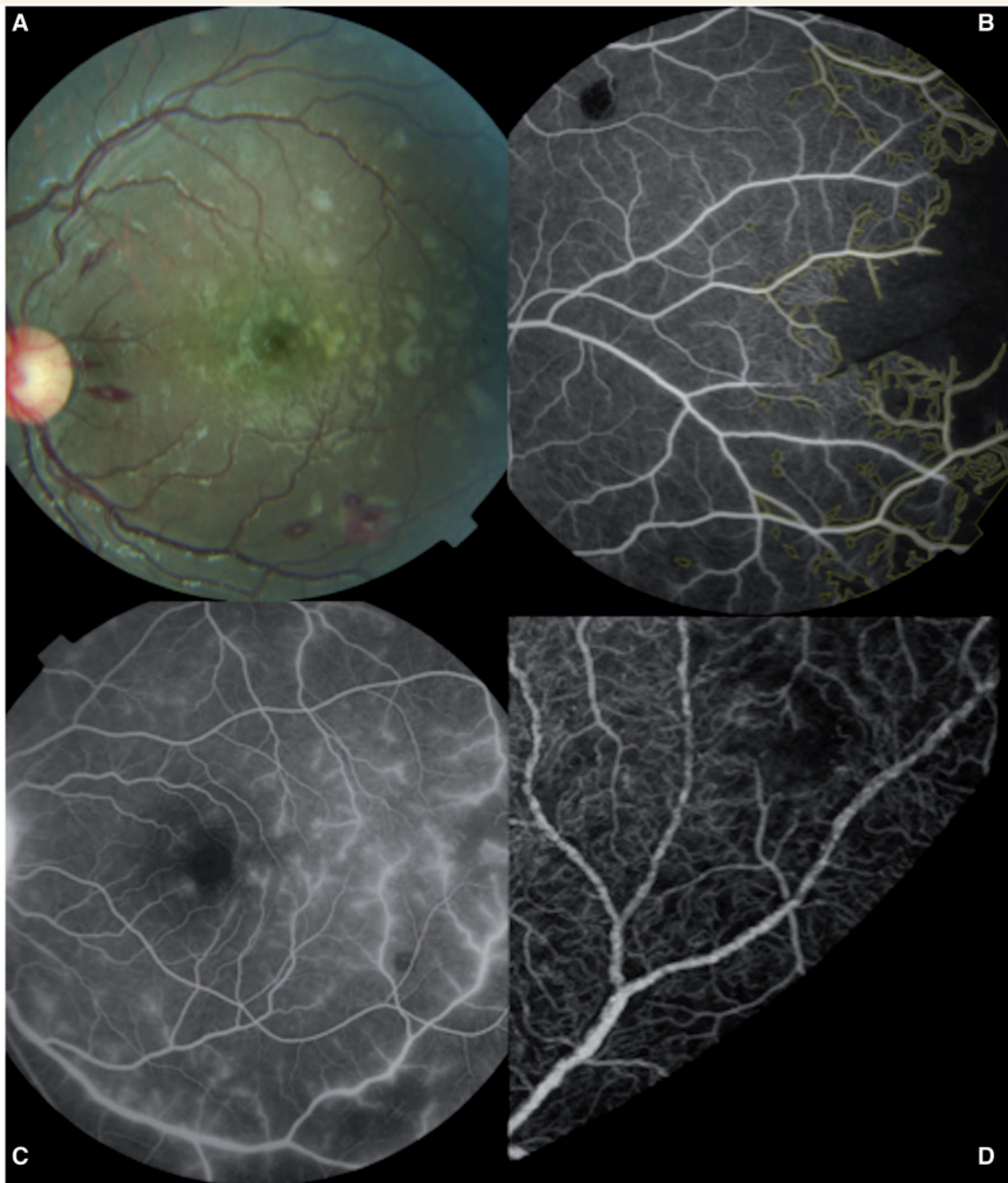


Figure 1 The features of paediatric malarial retinopathy are: retinal haemorrhages (often white-centred), retinal whitening, and orange or white discoloration of vessels. Papilloedema is often seen but is not specific for cerebral malaria. Angiographic signs include capillary non-perfusion, vessel mottling, and leakage. (A) Colour retinal image showing white-centred haemorrhages and retinal whitening extending from the macula into the temporal periphery (horizontal raphe). (B) Fluorescein angiography shows severe capillary non-perfusion in the retinal periphery (marked in yellow). Capillary non-perfusion typically coincides with retinal whitening. (C) Leakage of fluorescein from retinal venules. (D) Vessel mottling can be seen on a magnified fluorescein angiogram image. Images are from different subjects.

Areas of pale retinal discoloration are seen in other retinal conditions including arterial occlusion, venous occlusion (Browning, 2004), and Purtscher's retinopathy (Agrawal and McKibbin, 2006). Mild whitening has also been reported in paediatric severe malaria without coma (Beare *et al.*, 2004; Burton *et al.*, 2004). The severity and pattern of whitening seen in malarial retinopathy—around the fovea and extending into the horizontal

raphe—appears to be specific to cerebral malaria. Whitening in retinal vein occlusion is associated with swelling of the inner nuclear and outer plexiform layers of the retina (Sarda *et al.*, 2011). In paediatric cerebral malaria there is a significant inverse correlation between electroretinographic cone b-wave amplitude and severity of retinal whitening (Lochhead *et al.*, 2010), indicating dysfunction of bipolar cells in the inner nuclear layer. The inner

nuclear and outer plexiform layers are supplied by the deep capillary plexus, which forms the superficial half of a watershed with the underlying choriocapillaris (McLeod, 2010). This suggests that patterns of retinal whitening in cerebral malaria may correspond to venous congestion in areas with limited collateral drainage as well as high metabolic demand.

Retinal haemorrhages

The haemorrhages of malarial retinopathy are often white-centred. Retinal vessel thrombi are more common in fatal paediatric cerebral malaria than in coma of other cause. Microthrombi are sometimes associated with haemorrhage, but often occur independently (White *et al.*, 2009). White-centred haemorrhages also occur in bacterial endocarditis, leukaemia, and a range of other conditions in which capillary fragility and elevated venous pressure seem to be common factors (Duane *et al.*, 1980; Ling and James, 1998; Zehetner and Bechrakis, 2011). Retinal haemorrhages have also been observed in children with severe malarial anaemia without profound coma, and severity seems to increase with decreasing consciousness (Beare *et al.*, 2004). In paediatric cerebral malaria, the number of retinal haemorrhages at autopsy correlates significantly with the number of brain haemorrhages (White *et al.*, 2001). Retinal haemorrhages usually involve the inner retinal layers, but can extend to all layers. Different locations within the retina give rise to the appearance of blot or flame haemorrhages. Subretinal haemorrhage with secondary retinal detachment is seen with unusually large retinal haemorrhages (White *et al.*, 2009).

Manifestations of cerebral malaria: paediatric retina and brain compared

Several similarities exist between paediatric retina and brain vascular pathology (Table 1).

Microvascular sequestration is a defining histopathological feature of paediatric cerebral malaria in both retina and brain, and is thought to be the principal cause of tissue injury in both sites. Whenever brain and retinal histology has been compared in cases of fatal paediatric cerebral malaria, brain sequestration is always associated with retinal sequestration (Lewallen *et al.*, 2000; White *et al.*, 2009). On the other hand retinal vessel discolouration is not seen in fatal coma of other cause, implying absence of retinal sequestration in these cases (White *et al.*, 2009). Sequestration appears to be patchy within microvascular networks of each organ, but is more widespread in brain than retina.

Whereas the density of sequestration in paediatric cerebral malaria appears to be roughly equal between cerebral white and grey matter, cerebellum and brainstem (Armah *et al.*, 2005), the distribution and density of sequestration in the eye as a whole has not yet been formally evaluated. Pilot data from a small number of eyes from children with cerebral malaria suggest that both the percentage of parasitized vessels and the intensity of sequestration

are higher in the retina than in the adjacent choroid (Hiscott and Barrera, unpublished observations).

The intensity of tissue specific sequestration within the eye might be explained by the distribution of endothelial receptors in different vascular beds. ICAM1 is constitutively expressed by retinal vascular and choroidal endothelium at low levels (Duguid *et al.*, 1992), and in the choriocapillaris expression is greatest at the macula (Mullins *et al.*, 2006). Expression of retinal endothelial ICAM1 increases in infectious (*Toxoplasma gondii*) (Smith *et al.*, 2007) and non-communicable diseases (Funatsu *et al.*, 2005), and in response to vascular endothelial growth factor (Lu *et al.*, 1999).

Physiological differences between retinal and choroidal vascular beds may also influence sequestration, as they differ significantly in terms of capillary width, blood flow volume and oxygen extraction. In isolated rat microvessels sequestration density is inversely related to venule diameter, suggesting flow velocity and shear rate may be important (Kaul *et al.*, 1991). Several authors suggest that microvascular architecture may contribute to differential sequestration rates in various organs (Spitz, 1946; Nagatake *et al.*, 1992; Sein *et al.*, 1993).

White-centred and ring haemorrhages are common in the retina and brain, respectively. Presumably ring haemorrhages are spherical before histopathological sectioning, which like retinal imaging, provides a 2D view of the observed tissue. The haemorrhages of paediatric cerebral malaria generally affect inner retinal layers and cerebral white matter. In both sites long vessel segments are present, and these may be important in determining the localization of haemorrhages (Spitz, 1946). Clinically, haemorrhages in malarial retinopathy may occur without white centres (i.e. blot haemorrhages), or may develop white centres over time. At histopathology retinal haemorrhages often appear similar to ring haemorrhages—centred on a small thrombosed vessel with a halo of non-parasitized erythrocytes (White *et al.*, 2009). Variations in appearance result from the histological section and differences between retinal and cerebral cellular architecture.

Some areas of retina and brain appear to be affected more frequently by perfusion abnormalities than others. In the retina, fluorescein angiogram imaging suggests that watershed regions such as the horizontal raphe and margin of the foveal avascular zone are especially susceptible to capillary non-perfusion (Beare *et al.*, 2009). In the brain, patterns of T₂ and diffusion-weighted imaging signal changes on MRI (Potchen *et al.*, 2012) could represent boundaries of venous territories. Analysis of venous watershed regions in retina and brain may identify vessel properties that are important for the microvascular pathogenesis of cerebral malaria.

Haemorheology and neurovascular manifestations of cerebral malaria

Blood flow characteristics such as viscosity, haematocrit, and shear stress are relevant to paediatric cerebral malaria because they are likely to influence both the delivery of parasitized erythrocytes to

organ regions and the propensity for adherence to the endothelium and other erythrocytes. Shear stress strongly influences endothelial binding, for both leucocytes (Xu *et al.*, 2003; Crane and Liversidge, 2008) and parasitized erythrocytes (Fedosov *et al.*, 2011b), and is related to the deformability of parasitized and uninfected erythrocytes in severe adult falciparum malaria. Admission erythrocyte deformability is reduced in adult severe malaria compared with uncomplicated cases, and is associated with mortality (Dondorp *et al.*, 1997). Platelet mediated auto-agglutination (clumping) of erythrocytes is also associated with severity of malaria in adults (Pain *et al.*, 2001; Chotivanich *et al.*, 2004)

The movement of blood in small vessels is complex and depends on the character of blood and the vascular network it flows through. Unlike water (a Newtonian fluid), blood is a suspension of cells in plasma, and is an example of a shear thinning non-Newtonian fluid. The movement of blood in small vessels therefore varies with viscosity, haematocrit, blood cell deformability, aggregation and interaction with the endothelium (Schmid-Schönbein, 1999; Baskurt and Meiselman, 2003; Lipowsky, 2005; Popel and Johnson, 2005).

Blood viscosity decreases with increasing shear rate (Fig. 2), and as shear rate is related to blood velocity and vessel width, blood moves more easily at greater velocities and in vessels of lower calibre (Baskurt and Meiselman, 2003). Erythrocyte aggregation and deformation are major determinants of shear thinning (Popel and Johnson, 2005), and both are altered in *P. falciparum* infection (Dondorp *et al.*, 1997; Pain *et al.*, 2001; Chotivanich *et al.*, 2004; Fedosov *et al.*, 2011b). Erythrocyte stiffness is particularly important under high shear conditions, whereas non-streamlined aggregates increase resistance at low shear rates that are insufficient to break bonds between erythrocytes (Baskurt and Meiselman, 2003). Consistent with this, experimentally induced rosetting of *P. falciparum* infected erythrocytes is seen in venules, but not arterioles where shear rates are likely to be higher (Kaul *et al.*, 1991). Besides shear rate, viscosity depends on the volume fraction of erythrocytes in plasma (i.e. haematocrit). Rising haematocrit is associated with an exponential increase in viscosity.

Variable viscosity

Under normal conditions blood viscosity decreases as vessel width reduces. This phenomenon is known as the Fåhræus-Lindqvist effect, and is thought to result from migration of erythrocytes away from the vessel wall and into a central column—reducing resistance to flow by creating a lubricating cell-depleted layer next to the endothelium. Apparent viscosity reaches a minimum at an internal diameter of 5–7 μm (close to erythrocyte dimensions: $\sim 6\text{--}8\ \mu\text{m}$ diameter, $2\ \mu\text{m}$ thick) after which it rises steeply (Popel and Johnson, 2005). Apparent viscosity is greater *in vivo* than in equivalent glass tubes of the same internal diameter, and this is thought to result from resistance to flow produced by an endothelial lining (the endothelial surface layer or glycocalyx) (Pries *et al.*, 2000; Popel and Johnson, 2005). Protrusion of endothelial cell pseudopods into the vessel lumen during endothelial activation can almost double capillary resistance to flow (Schmid-Schönbein, 1999), and sequestered erythrocytes, or associated inflammation, may produce a similar effect.

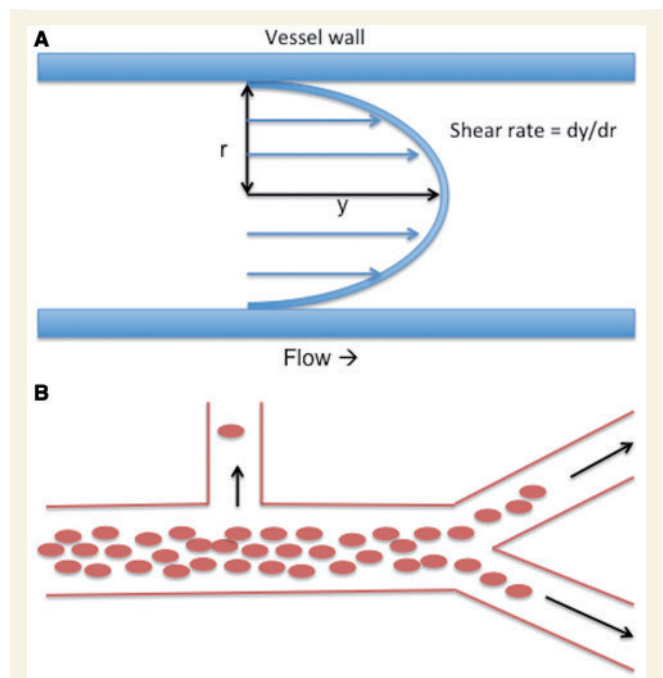


Figure 2 (A) Illustration of shear rate in parabolic (laminar) flow. Shear rate is a function (dy / dr) of flow velocity (y) and vessel width (r). At a given velocity shear rate is greater in narrow vessels than wide vessels. Blood is a shear thinning fluid, meaning that blood viscosity decreases with increasing shear rate. Shear stress is the product of viscosity and shear rate. (B) Phase separation with heterogeneous haematocrit in vessel branches. Variable haematocrit arises when erythrocytes are distributed unevenly as a result of phase separation. Erythrocytes flow in a central column surrounded by a cuff of plasma. The proportion of erythrocytes to plasma in vessel branches depends on branching angle, daughter vessel width, and daughter vessel flow rate. Daughter vessels branching at near 90° have a relatively high proportion of plasma and therefore lower haematocrit than the parent vessel.

Erythrocytes are by far the most common suspended component of blood, and so under physiological conditions, local haematocrit and shear rate are the major determinants of apparent viscosity in microvessels (Lipowsky, 2005). Leucocytes make up a relatively small fraction of total blood volume ($\sim 1/600$). Nonetheless, as a typical inactivated neutrophil is $\sim 8\ \mu\text{m}$ wide, temporary obstruction of capillaries (internal diameter $4\text{--}8\ \mu\text{m}$) is common, and leucocytes can increase resistance to blood flow within an organ even without binding to endothelium, depending on leucocyte count, haematocrit and the capillary length of the organ involved. The effect is greater in organs with long capillary segments than in those with short segments such as the pulmonary circulation, and probably results from reductions in capillary erythrocyte velocity to match that of the slower leucocytes (Schmid-Schönbein, 1999). Leucocytes, which are relatively large and stiff, also strip the endothelial surface layer from capillary endothelium as they pass. This effect may persist into post-capillary venules and result in increased exposure of endothelial receptors such as ICAM1 (Popel and Johnson, 2005), presumably

facilitating endothelial binding and subsequent migration through the vessel wall. Parasitized erythrocytes are similar to leucocytes in that they are relatively stiff and bind to ICAM1 (Fedosov, *et al.*, 2011a; Moxon *et al.*, 2011), and this may contribute to microvascular congestion, whereas exposure of capillary and post-capillary endothelial receptors as a result of stripping of the endothelial surface layer may be an important step in sequestration. Post-capillary venules may favour sequestration because shear stress is lower than in arterioles (Nagaoka and Yoshida, 2006). Microvascular resistance is likely to be raised by high proportions of inflexible erythrocytes, sequestration and auto-agglutination, leading to reduced velocity, increased viscosity, and lower shear stress. Increased viscosity can have a dramatic effect on the retinal circulation, and ultimately lead to venous stasis or occlusion (Pournaras *et al.*, 2008). Congestion and blockage of venules and capillaries secondary to high blood viscosity is therefore consistent with clinical signs of malarial retinopathy such as haemorrhage and capillary non-perfusion.

Variable haematocrit

Local microvascular haematocrit is not the same as systemic haematocrit. The haematocrit of blood flowing into a small tube is significantly less than that measured in the static effluent exiting the tube. This is known as the Fåhræus effect, and—as with the Fåhræus–Lindqvist effect—is thought to result from the tendency of flowing erythrocytes to migrate axially to form a central column (Lipowsky, 2005; Popel and Johnson, 2005).

Microvessel haematocrit is not distributed evenly between vessels. When blood meets a bifurcation there is unequal division of erythrocytes into the daughter vessels. Distribution depends on parent vessel haematocrit, branching angle and daughter vessel flow rates. Flow rate is especially influential. This effect is known as phase separation and, again, is thought to result from the axial position of erythrocytes (Fig. 2). As a result microvessel haematocrit is heterogeneous across a network (Popel and Johnson, 2005; Hirsch *et al.*, 2012), and can show great variation (Ganesan *et al.*, 2010; Guibert *et al.*, 2010). As haematocrit is a major determinant of blood viscosity, the concept of phase separation and heterogeneous haematocrit within microvascular networks is crucial to understanding the possible role of haemorheological factors in the retinal and cerebral manifestations of retinopathy-positive paediatric cerebral malaria.

Computational models of blood flow

The close relationship between haemorheology and microvascular architecture means that computational models of flow parameters can be extended from single vessels to entire networks. Models exist for mouse retina (Ganesan *et al.*, 2010) and primate cerebral cortex (Guibert *et al.*, 2010). The mouse model predicts high regional haematocrit in the retinal periphery, but varying up to a factor of four, likely owing to phase separation. Predicted viscosity is greatest in capillaries and peri-capillary vessels, but can also vary significantly (by a factor of three) owing to heterogeneous local haematocrit. Shear stress is lower in venules than arterioles of the same size, and again reduces towards the peripheral retina for

vessels of a given width (Ganesan *et al.*, 2010). Distribution of more erythrocytes to the retinal periphery than to the posterior pole may be important physiologically, because oxygen delivery depends on blood viscosity as well as on haematocrit (Cho and Cho, 2011). It may be that the macula benefits from greater oxygen transfer as a result of lower regional viscosity compared to the retinal periphery.

Estimations from the mouse are unlikely to correspond exactly to the human retina. However, the haemorheological principles behind the model may help to explain some features of malarial retinopathy. For example the peripheral retina may develop large zones of capillary non-perfusion that cut across arterioles and venules, while macular capillary non-perfusion tends to affect smaller patches of capillaries (Beare *et al.*, 2009) (Fig. 1B). This may be because greater parasite delivery to the periphery promotes occlusion of wider vessels, compared to the macula, which has higher metabolic demands but lower microvascular haematocrit.

The relationship between flow and microvascular networks in paediatric cerebral malaria

In summary, haemorheological factors may both influence and be influenced by *P. falciparum*. For example, organ regions with physiologically high microvascular viscosity and low shear stress may be especially susceptible to sequestration, while *P. falciparum*-associated erythrocyte stiffness, auto-agglutination and sequestration are likely to increase viscosity. As well as factors arising from blood itself, predisposition of microvascular regions to high or low haematocrit and viscosity depends on vessel network architecture. The combination of physiological heterogeneity within microvascular networks, which is influenced by network architecture, and pathological derangements of blood movement caused by *P. falciparum*, may help to explain manifestations of cerebral malaria in retina and brain. If so, common neurovascular network architecture could contribute to a biologically plausible rationale for inferring unseen cerebrovascular pathogenesis from the visible retina. Therefore we now compare retinal and cerebral microvasculature geometry and topology (Table 2).

The retina

Retinal microvasculature

The retina has a dual blood supply. The inner retinal circulation supplies the visible inner surface of the retina. The choroidal circulation, lying between the retinal pigment epithelium and sclera, supplies the outer retina, including the photoreceptors (Hayreh, 2010a; McLeod, 2010). Retinal and choroidal circulations have major differences in anatomy and physiology. The choroid is made up of an outer layer of large vessels (Haller's layer), a middle layer of smaller vessels (Satler's layer), and an innermost layer of capillaries (the choriocapillaris). The range of capillary width in the choriocapillaris is large compared to inner retina (3–50 μm versus 3.5–6 μm) (Anand-Apte and Hollyfield, 2010). Although anatomical studies classically suggested that the

Table 2 Comparing vascular features between retina and brain that are likely to be important in cerebral malaria pathogenesis

Area of comparison	Similarities / differences	Discussion
Vascular geometry	Similarities	First and second generation retinal arterioles are ~100- μ m wide (Nagaoka and Yoshida, 2006), deep white matter arterioles are 100 to 170- μ m wide (Nonaka <i>et al.</i> , 2003b), arterioles in the putamen are ~100 to 150- μ m wide (Nonaka <i>et al.</i> , 1998). Retinal perifoveal capillaries are ~5.4- μ m wide (Wang <i>et al.</i> , 2011), cerebral grey matter capillaries are ~6.5- μ m wide (Lauwers <i>et al.</i> , 2008), capillaries in the putamen ~5 to 7- μ m wide (Wolfram-Gabel and Maillot, 1994). The largest retinal venules are 130- μ m to 150- μ m wide (Nagaoka and Yoshida, 2006), cerebral grey and white matter venules range up to 125 μ m (Duvernoy <i>et al.</i> , 1981). Retina (Pournaras <i>et al.</i> , 2008), cerebral grey (Cassot <i>et al.</i> , 2010) and white matter (Figs 7 and 9 in Nonaka <i>et al.</i> , 2003b) all have ~90° branches from relatively long straight trunks. Caudate and putamen have retrograde arteriolar branching. Basal ganglia venous branches join at right angles (Nonaka <i>et al.</i> , 1998).
	Differences	First generation retinal arterioles are ~100- μ m wide (Nagaoka and Yoshida, 2006), cerebral grey matter penetrating arterioles are 20- to 65- μ m wide (Duvernoy <i>et al.</i> , 1981; Reina-de La Torre <i>et al.</i> , 1998). The largest retinal venules are 130- to 150- μ m wide (Nagaoka and Yoshida, 2006), principal veins in the putamen can be up to ~500- μ m wide (Wolfram-Gabel and Maillot, 1994). Retinal arteriolar and venular length between bifurcations is similar to the length of entire penetrating arterioles or venules in grey matter.
Vascular topology	Similarities	Strahler order in the macula is ~3.5, in cerebral grey matter it is 3 to 5 (Cassot <i>et al.</i> , 2010; Yu <i>et al.</i> , 2010). Capillary density immediately around the human foveal avascular zone is similar to primate cortex (Tam <i>et al.</i> , 2010).
	Differences	Human macular superficial and deep plexus have density 40% and 20% per unit area, whereas human grey matter has density ~1.5 to 2% brain volume (Cassot <i>et al.</i> , 2006; Lauwers <i>et al.</i> , 2008; Mendis <i>et al.</i> , 2010). Arteriole/venule ratio in retina is 1:1, in cerebral grey matter it is 2:1, in basal ganglia it is up to 5:1 (Wolfram-Gabel and Maillot, 1994; Cassot <i>et al.</i> , 2010).
Watershed regions	Similarities	Both brain and retina have arterial and venous watershed regions. Insufficient venous outflow can cause oedema, haemorrhage, and ischaemia in brain (Teksam <i>et al.</i> , 2008) and retina (Browning, 2004).
	Differences	Retinal arteriolar and venular watersheds tend to have the same distribution, e.g. the edge of the foveal avascular zone, and horizontal raphe. In the brain arteriolar and venular watersheds cover different anatomical territories (Miyawaki and Statland, 2003a, b). In the retina venous drainage almost always follows arterioles. Variation in cerebral venous drainage is common in children (Widjaja and Griffiths, 2004).
Metabolic demand	Similarities	Metabolic demand per unit tissue for retina and brain is comparable, and higher than any other organ (Wong-Riley, 2010). Both retina and brain depend on a constant supply of oxygen and glucose (Mckenna <i>et al.</i> , 2006). Both inner retina and brain vessels have an arterio-venous O ₂ difference of ~40–50% (McLeod, 2010; Seifert and Secher, 2011). Retinal metabolism is greatest around the fovea and in retinal layers rich in synapses (Yu and Cringle, 2001; Birol <i>et al.</i> , 2007). Cerebral metabolism is greater in grey matter than white matter (Sokoloff, 2003).
	Differences	Cerebral metabolic demand peaks in childhood: cerebral metabolic rate for O ₂ is 4.3 to 6.2 ml O ₂ /100 g/min (3 to 6 years, whole brain) (Kennedy and Sokoloff, 1957); cerebral metabolic rate for glucose is >30 μ mol/100 g/min (1 to 2 years, calcarine cortex, transverse temporal cortex, lenticular nuclei) (Chugani <i>et al.</i> , 1987). It is not clear if retinal metabolic demand changes significantly after birth.
Blood flow	Similarities	Both retina and brain receive high blood flow volume per unit tissue.
	Differences	Inner retinal blood flow volume is roughly half that of the adult brain (25:50 ml/100 g/min, inner retinal circulation to total brain) (Kety and Schmidt, 1948; Madsen <i>et al.</i> , 1993; Sokoloff, 2003; Pournaras <i>et al.</i> , 2008). Cerebral blood flow is much higher in early childhood compared with adulthood (130 ml/100 g/min, age 2 to 4 years) (Wintermark <i>et al.</i> , 2004). It is not clear if retinal blood flow undergoes similar changes in childhood. Paediatric peak systolic cerebral blood flow velocity is ~95 cm/s in the middle cerebral artery and ~4.5 cm/s in the central retinal artery (Geeraerts <i>et al.</i> , 2005).

choroid has multiple anastomoses, *in vivo* functional imaging reveals end-arterial segmental perfusion with associated watershed regions (Hayreh, 1990, 2010b). In the macaque, choroidal blood flow volume is roughly 20 times greater than in the retina, and nine times greater than cerebral grey matter, per weight of tissue (Alm and Bill, 1973; Hayreh 2010b). Wide capillaries and high volumetric flow rate may help to explain why the choriocapillaris is less

susceptible to sequestration than inner retinal vessels (Hiscott and Barrera, unpublished observations).

Geometry of the inner retinal circulation

The central retinal artery usually divides to produce four branches that extend from the optic disc into the four quadrants of the

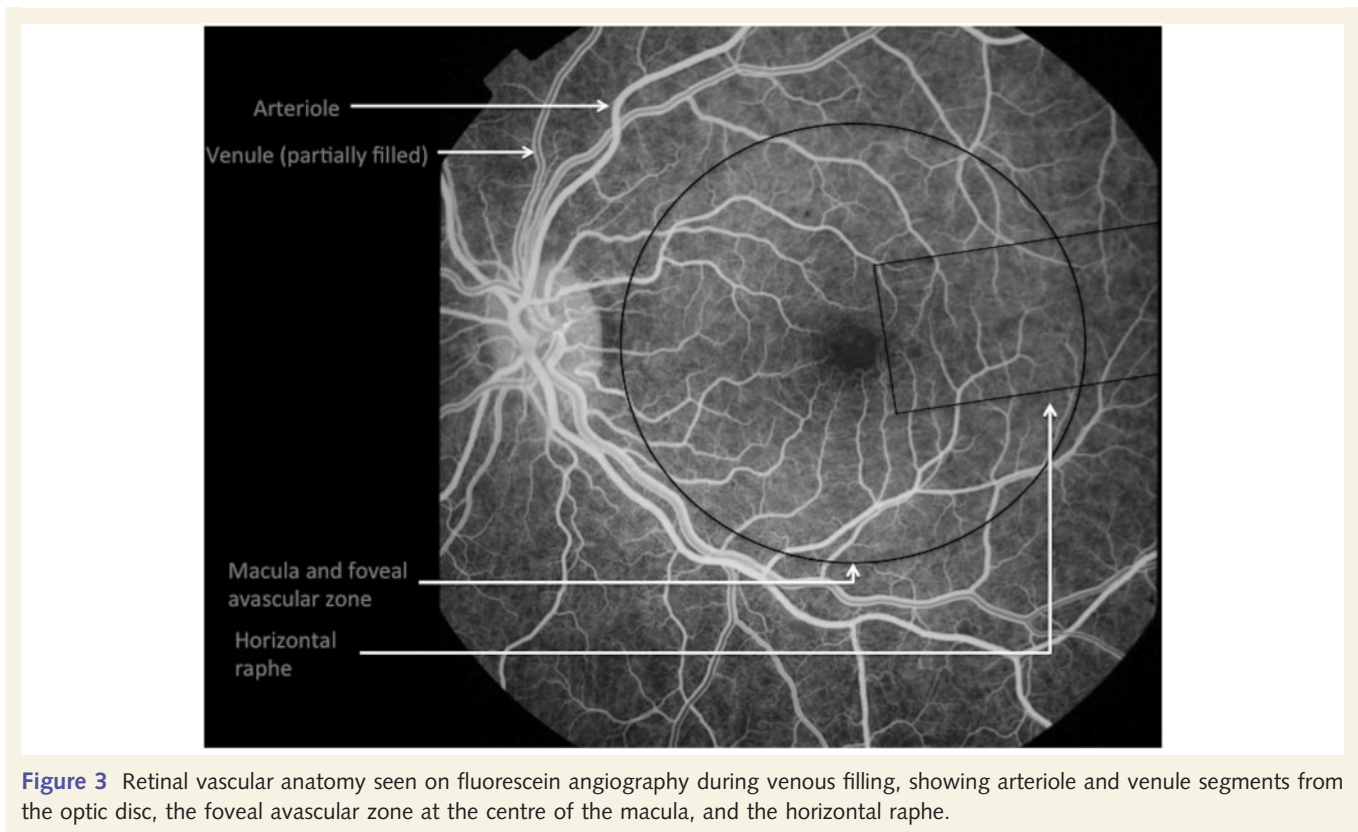


Figure 3 Retinal vascular anatomy seen on fluorescein angiography during venous filling, showing arteriole and venule segments from the optic disc, the foveal avascular zone at the centre of the macula, and the horizontal raphe.

retina (Fig. 3). Further branching is either at right angles to the main trunk or dichotomous (i.e. two daughter branches at approximately right angles to each other) (Berntson, 1995; Pournaras *et al.*, 2008).

In healthy adults the central retinal artery is $\sim 160 \mu\text{m}$ wide (Dorner *et al.*, 2002). First and second generation arterioles are $\sim 100 \mu\text{m}$ wide, whereas first and second-generation venules are ~ 150 and $130 \mu\text{m}$, respectively (Nagaoka and Yoshida, 2006). Retinal arteriolar cross sectional profiles tend to be circular, whereas venule lumens may be circular but tend to collapse (Feke *et al.*, 1989).

Vascular segments extend close to the anterior limit of the retina, leaving a peripheral avascular zone $\sim 1.5 \text{ mm}$ wide. Each terminal arteriole gives rise to a network of 10 to 20 interconnected capillaries (Hayreh, 2010a). Capillary arrangement varies between retinal locations. In general there are two layers: a superficial plexus between the nerve fibre layer and ganglion cell layer, and a deep plexus between the inner nuclear and outer plexiform layers (McLeod, 2010). Only one layer exists adjacent to the fovea and at the far periphery. The peripheral network is also relatively sparse. In the peripapillary region a third capillary layer extends radially from the optic disc for a distance of up to several millimetres (Hayreh, 2010a).

Capillaries are absent at the foveal avascular zone, and adjacent to retinal arterioles (Fig. 3). The foveal avascular zone is supplied by diffusion from the underlying choriocapillaris and in adults is $\sim 400 \mu\text{m}$ wide and $350 \mu\text{m}$ high (Yu *et al.*, 2010). Periarteriolar capillary free zones are between 50 and $120 \mu\text{m}$ wide (Kuwabara and Cogan, 1960). They reflect the combined radius of oxygen diffusion from both artery segment and adjacent capillaries. Capillary-free zones are narrower next to venules, reflecting the high oxygen

extraction ($\sim 50\%$) of the retinal circulation and reducing oxygen diffusion radius from post-capillary venules (McLeod, 2010).

Draining venules rise obliquely from the capillary plexuses to the nerve fibre layer and combine to form vascular patterns similar to retinal arterioles. Venules are generally slightly wider than arterioles, with shorter distances between bifurcations, narrower branching angles and less tortuosity (Hughes *et al.*, 2009). Postcapillary venules interdigitate with precapillary arterioles in an alternating pattern (Bek and Jensen, 1993); this can become strikingly apparent in malarial retinopathy when leakage affects venules more than arterioles (Beare *et al.*, 2009) (Fig. 1C). Venules follow arterioles to converge at the optic disc, where they drain into the central retinal vein. Venous blood from the inner retina then flows into the cavernous sinus, either directly or by way of the superior ophthalmic vein. There are no valves (Hayreh, 2010a; Semmer *et al.*, 2010).

Some information exists about vessel geometry in children (Table 3). Paediatric central retinal artery equivalent and central retinal vein equivalent are calculated values based on the widths of first generation retinal vessels, and seem to be similar to adult values. Arteriolar bifurcation angle (the angle subtended between two branches from a parent arteriole) seems to be greater in children than adults, as does arteriolar length to diameter ratio. It is not clear how these differences might affect sequestration.

The macula

The macula is a unique region within the CNS situated temporally to the optic disc and specialized for fine resolution colour vision.

Table 3 Retinal vessel geometry in children and adults

Measurement	Children				Adults			
	Age	n	Value	Reference	Age	n	Value	Reference
Central retinal artery equivalent	7–9 y	760	156.4 (155.4–157.3) μm ; mean (95% CI)	Cheung <i>et al.</i> , 2007	43–86 y	4231	165.29 (15.42) (98.1–223.4) μm ; mean (SD) (range)	Lee <i>et al.</i> , 2004
0.5–1.0 DD from optic disc margin	9 y	266	168.41 (14.82) μm ; mean (SD)	Sun <i>et al.</i> , 2009	43–86 y	4231	242.08 (22.86) (165.1–352.9) μm ; mean (SD) (range)	Lee <i>et al.</i> , 2004
	4–6 y	385	159.08 μm (mean of groups)	Li <i>et al.</i> , 2011				
	6 y	1612	163.2 (14.0) μm ; mean (SD)	Rochtchina <i>et al.</i> , 2008				
	6 y	1608	163.3–166.9 μm (range)	Taylor <i>et al.</i> , 2007				
Central retinal vein equivalent	7–9 y	760	225.4 (224.1–226.8) μm ; mean (95% CI)	Cheung <i>et al.</i> , 2007				
0.5–1.0 DD from optic disc margin	9 y	266	247.48 (18.99) μm ; mean (SD)	Sun <i>et al.</i> , 2009	45–75 y	167	69.5° (64.5–78.3°); median (range)	Hughes <i>et al.</i> , 2009
	4–6 y	385	222.12 μm (mean of groups)	Li <i>et al.</i> , 2011				
	6 y	1612	227.3 (18.3) μm ; mean (SD)	Rochtchina <i>et al.</i> , 2008				
	6 y	1608	228.8–234.8 μm (range)	Taylor <i>et al.</i> , 2007				
Arteriolar bifurcation angle	12 y	263	78.63° (mean of groups)	Tapp <i>et al.</i> , 2007				
Arteriolar simple tortuosity	12 y	263	0.025 (mean of groups)	Tapp <i>et al.</i> , 2007				
Arteriolar length to diameter ratio	12 y	263	13.1 (mean of groups)	Tapp <i>et al.</i> , 2007				

Several subregions exist within the macula, for which adult vessel topology has been described (Yu *et al.*, 2010). Macular arterioles and venules are paired, with an average of nine pairs converging radially towards the fovea. Only three pairs enter the fovea itself to supply the terminal capillary ring marking the edge of the foveal avascular zone. Macular capillaries arise at right angles from parent arterioles and venules (Yu *et al.*, 2010)—an arrangement consistent with significant phase separation and variation in viscosity. Mean perifoveal capillary width has been measured at 5.4 μm using ultra-high resolution optical coherence tomography (Wang *et al.*, 2011). These capillaries are slightly narrower than capillaries in post-mortem sections of human temporal cortex (6.5 μm) (Lauwers *et al.*, 2008).

The retinal periphery

At the far periphery arterioles form looping arcades with adjacent venules, which may also be traversed by bridging vessels. Trypsin digest reveals peripheral loops with a diameter greater than capillaries at the posterior pole (up to 30 μm versus 5 μm). This arrangement varies between quadrants within eyes, and between individuals (Spitznas and Bornfeld, 1977). If retinal haematocrit is indeed concentrated towards the periphery, these vessels may facilitate flow of blood with relatively higher viscosity than found at the macula. These vascular features are visible in fluorescein angiogram images in paediatric subjects (Penman *et al.*, 1994), though the optical properties of the eye mean that appearances on fluorescein angiogram are likely to be magnified compared to histopathology. In malarial retinopathy normal arteriovenous loops should not be confused with capillary non-perfusion in the far periphery.

Topology of inner retinal vessels

Topological measurements exist for the human macula and fovea. Using the generation number and Strahler taxonomy schemes, average macular branching generation for both arterioles and venules is ~ 11.5 , and average Strahler vessel order is ~ 3.5 . This indicates a high number of bifurcations from each arteriole and venule within a relatively short vessel segment length (Yu *et al.*, 2010). Strahler order in human cerebral grey matter is 3 to 5 (Cassot *et al.*, 2010).

Macular capillary density 1500 μm from the centre of the foveal avascular zone is $\sim 40\%$ in the superficial capillary network and 20% in the deep network, calculated as percentage of sample area filled by vessel segments (Mendis *et al.*, 2010).

The relatively sparse capillary network encircling the foveal avascular zone has been quantified as total capillary length/sample area. Average density ranges from 30 to 34 mm/mm^2 (Tam *et al.*, 2010). Direct comparison of 2D retinal area with 3D brain volume is difficult, but capillary density in the human brain has been measured at $\sim 250 \text{mm}/\text{mm}^3$ (visual cortex) (Bell and Ball, 1985).

Watershed regions

Excepting arteriovenous loops in the far periphery, the absence of arterial, venous, and arteriovenous anastomoses means that there

are several watershed zones in the inner retinal circulation (Fig. 3). These exist between:

- (i) Terminal vessels of each of the four arcades, most notably the superior and inferior temporal branches where they form the horizontal raphe;
- (ii) Vessels of the retina and vessels of the ciliary body at the anterior limit of the retina; and
- (iii) The deep capillary plexus and choriocapillaris throughout the retina, because there is no communication between the inner retina and the choriocapillaris. As the foveal avascular zone is supplied solely by the choriocapillaris this watershed is demarcated clinically in central retinal artery occlusion as the edge of the classic 'cherry red spot'.

It is important to note that arterial and venous watersheds in the retina are identical, because of pairing of arterioles and venules. This is not the case in the brain, where arterial and venous territories are different.

Retinal metabolism and blood flow

The retina is considered by many to be the most metabolically active tissue in the body (Wong-Riley, 2010; Kur *et al.*, 2012). High demands may put it at greater risk of ischaemia in cerebral malaria. Perifoveal oxygen consumption at the dark-adapted macaque is 4.9 ml/100 g/min (Birol *et al.*, 2007). Retinal oxygen consumption in man is estimated at 9.7 ml O₂/100 ml retina/min (Anderson and Saltzman, 1964) or ~10 ml O₂/100 g retina/min (assuming retinal specific gravity of 1.0425) (Stefánsson *et al.*, 1987), compared with ~3 ml/100 g/min for brain (Kety and Schmidt, 1948; Madsen *et al.*, 1993; Sokoloff, 2003). In the macaque, retinal glucose consumption is among the highest in the CNS (Sperber and Bill, 1985). Estimates of energy expenditure based on ATP used per neuron suggest the human retina may consume ~11.75 mW/g, and the human brain ~10.5 mW/g (assuming retinal weight = 0.4 g, retinal energy = 4.7 mW; brain weight = 1400 g, brain energy = 14.6 W) (Sarpeshkar, 2010).

Only a small proportion of blood from the ophthalmic artery goes to the inner retinal circulation. The value often reported is ~4% (Williamson and Harris, 1994; Pournaras *et al.*, 2008). It is not clear if this figure is from human or animal studies, but for comparison Alm and Bill (1973) found that retinal flow in the macaque makes up ~3.3% of blood to the retina and uvea combined (~27/811 mg/min). Consequently, inner retinal blood flow volume is a small fraction of ocular flow, which is itself a small fraction of blood flow in the internal carotid artery.

In non-human mammals, the retinal layers with highest metabolic rate are the inner segments of the photoreceptors, the outer plexiform layer, and the deeper region of the inner plexiform layer (Yu and Cringle, 2001). Oxygen reaches these layers by diffusion from the choriocapillaris (photoreceptor inner segments), and deep capillary plexus (outer plexiform and deep inner plexiform layers) (McLeod, 2010). In the macaque, demand for oxygen is highest at the perifovea (Birol *et al.*, 2007), and is likely to decrease towards the periphery where photoreceptor density is substantially lower (Jonas *et al.*, 1992). Patterns of metabolic demand may influence

the susceptibility of neuronal tissue to the effects of sequestration, and resulting manifestations of malarial retinopathy. Retinal whitening is common in the highly metabolically active perifovea.

Measurements of human mean blood flow volume in the inner retinal circulation have been made using laser Doppler flowmetry, and vary between studies from ~30 to 80 µl/min/retina (reviewed in Pournaras *et al.*, 2008), which is ~9 to 25 µl/100 mg/min, assuming a human retinal weight of 326 mg (Feke *et al.*, 1989). The wide range may result from methodological differences. For comparison, inner retinal blood flow in the macaque, measured by radioactive microspheres, is ~18 µl/100 mg/min (assuming specific gravity of blood = 1.06 and macaque retinal weight of 128 mg) (Alm and Bill, 1973; Feke *et al.*, 1989).

In humans retinal blood flow volume is likely to be approximately half that of the brain, by tissue weight (i.e. 25:50 ml/100 g/min, inner retinal circulation to total brain) (Sokoloff, 2003; Pournaras *et al.*, 2008).

Mean perifoveal capillary flow velocity ranges from 1.37 to 3.3 mm/s. Leucocyte movement is pulsatile, and velocity in perifoveal vessels 7–11 µm wide is ~1.4 mm/s (Pournaras *et al.*, 2008). Rather than passing equally through all capillary segments perifoveal leucocytes seem to follow preferred pathways (Tam *et al.*, 2011). Similar patterns may exist for the movement of parasitized erythrocytes.

Estimated shear stress in healthy adults is highest in first generation arterioles (mean 54.0 dyne/cm²), 20% lower in second-generation arterioles, and 50% lower in both first and second-generation venules (Nagaoka and Yoshida, 2006; Nagaoka *et al.*, 2009).

The brain

The circulation of the brain is substantially more complex than that of the retina. We give a brief overview before focusing in more detail on three brain areas typically involved in acute paediatric retinopathy-positive cerebral malaria: the basal ganglia, cerebral grey matter and cerebral white matter. All are affected significantly more often in children with retinopathy-positive cerebral malaria than in paediatric patients with cerebral malaria without retinopathy (Potchen *et al.*, 2012). Retinopathy could therefore reasonably be associated with vascular disease processes in these areas, if microvascular characteristics are similar in both organs.

Cerebral vasculature architecture and watershed regions

Carotid and basilar arteries supply the variably anastomotic Circle of Willis, which sends off branches including the anterior, middle and posterior cerebral arteries. Arterial territories are exclusive and vary between individuals (Miyawaki and Statland, 2003a). As in the retina, arterial territories become apparent clinically in thrombo-embolic arterial occlusion when infarction occurs up to the watershed of that arterial territory.

Unlike the retina where arterioles and venules cover identical territories, cerebral venous drainage does not parallel the arterial supply. Several classifications exist (reviewed by Nowinski, 2012), but essentially venous drainage can be understood in terms of

superficial and deep venous systems (Ono *et al.*, 1984; Oka *et al.*, 1985). Although venous anastomoses exist within each system, there is no physiological anastomosis between superficial and deep systems (Andeweg, 1996, 1999). They join at the torcula (confluens sinuum), where the straight sinus (draining the deep system) meets the superior sagittal sinus and transverse sinus (draining the superficial system) (Miyawaki and Statland, 2003b). Anatomy is variable but the superficial venous system includes several cortical veins and sinuses that drain the exterior cortex, ranging in average width from ~0.5 to 5.0 mm (Oka *et al.*, 1985). The deep system drains subcortical and periventricular structures such as the insular cortex and basal ganglia. The watershed between the superficial and deep venous systems lies between the periventricular and subcortical white matter (Andeweg, 1996). Ultimately venous blood leaves the cranial vault through the internal jugular or spinal veins, and a small number of emissary veins.

Major venous channels show significant variation (Miyawaki and Statland, 2003b). In a magnetic resonance venography series of healthy children the inferior sagittal sinus was not seen in 54%. The right or left of the following were absent in many cases (% cases absent): vein of Trolard (~80%), vein of Labbe (~50%), superficial petrosal sinus (66%), and inferior petrosal sinus (~33%) (Widjaja and Griffiths, 2004). Lack of major collateral channels would make associated brain regions more vulnerable to venous congestion in paediatric cerebral malaria. Variation in venous drainage could help to explain patterns of MRI signal changes in acute retinopathy-positive paediatric cerebral malaria in the same way that venous territories within the superficial system appear to influence the distribution of radiographic lesions in paediatric cerebral venous thrombosis (Meder *et al.*, 1994; Teksam *et al.*, 2008).

Vascular anatomy of the basal ganglia

The basal ganglia comprise several interrelated nuclei with different neuronal structures, vascular architectures, and embryological origins. The arterial supply of the basal ganglia arises mainly from the middle cerebral artery with some contributions from the anterior cerebral artery and anterior choroidal artery. Branches from the anterior cerebral and anterior choroidal arteries supply the head of the caudate nucleus and globus pallidus (Akima, 1993). Ten to 20 lenticulostriate arteries from the middle cerebral artery enter the putamen, where they spread out in a fan shape and divide into two to three branches, each ~100 to 150 μm wide. These form capillary networks within the putamen and cross the internal capsule to supply the caudate nucleus (Nonaka *et al.*, 1998).

The vasculature of the putamen and caudate nucleus is distinct from that of the globus pallidus, internal and external capsules. Branching arterioles (~50 μm wide) of the putamen may reflect back and coil around the parent vessel before branching further. Precapillary arterioles of the putamen are ~20 μm wide (Wolfram-Gabel and Maillot, 1994). Retrograde arteriolar branching is seen but it is not clear if this is a feature of old age or is universally present (Nonaka *et al.*, 1998). If the latter they could produce heterogeneous viscosity from phase separation in children. In the

globus pallidus, arterioles tend to be fewer and straighter, with no coiling. The end arteriolar branches (~40 μm wide) form arteriolar anastomoses as well as a capillary net (Wolfram-Gabel and Maillot, 1994).

The capillary networks of the putamen and caudate nucleus have a similar density to the cerebral grey matter (600–650 capillaries per mm^2 in a 30 to 40 μm mesh), whereas the capillary density of the internal capsule approximates that of the cerebral white matter. The globus pallidus has capillary density between these extremes (200–350 per mm^2 in a 60–80 μm mesh) (Wolfram-Gabel and Maillot, 1994; Nonaka *et al.*, 1998). Capillary density seems to be proportional to the density of synapses (Akima, 1993). Capillaries of the putamen are ~5–7 μm wide (Wolfram-Gabel and Maillot, 1994).

Venules and veins throughout the basal ganglia are generally wider than the arterial vessels, and smaller veins meet larger vessels at right angles (Nonaka *et al.*, 1998). In the putamen, five arterioles are typically arranged around a single central 'principal' vein, which together form a vascular unit. These veins can be large (~500 μm wide) (Wolfram-Gabel and Maillot, 1994). The high ratio of arterioles to veins suggests a similarity to cerebral cortical vessels, and an important difference with the retina where arterioles and venules are paired. Congestion of a principal vein is likely to have a disproportionate impact on perfusion. This may be relevant to cerebral malaria since sequestration is thought to occur in venules to a greater extent than arterioles, although it is not clear how often congestion occurs in venules up to 500 μm wide.

Vascular anatomy of the cerebral grey matter

Branches from the anterior, middle, and posterior cerebral arteries produce a network of pial arterioles on the cerebral surface. Cortical arterioles (~20 to 90 μm wide) branch from the pial vessels and travel on the brain surface for ~150 to 750 μm before turning 90° to penetrate the cortex (Reina-de La Torre *et al.*, 1998).

There are no capillaries on the brain surface, and the absence of arterio-venous anastomoses at this point means that all arterial blood is forced into penetrating cortical arterioles and the capillaries of the cerebral cortex (Duvernoy *et al.*, 1981).

Penetrating cortical arterioles reach depths of 150 μm to ~3 mm and have widths between ~20 and 65 μm . They branch to form capillaries and pre-capillary arterioles at several levels parallel with the brain surface. Mean arteriolar branching angle is 112 to 126°, depending on daughter vessel diameter (Cassot *et al.*, 2010). Some pre-capillary branches are recurrent (Duvernoy *et al.*, 1981; Reina-de La Torre *et al.*, 1998).

The topology of cortical vessel segments can be thought of in terms of 'tree-like' penetrating vessels and 'net-like' capillaries (Lauwers *et al.*, 2008). The tree-like arteriolar and venular segments have a long parent vessel 'trunk' from which smaller branches emanate (Cassot *et al.*, 2010), and are suited to rapid movement of blood, whereas the capillary net is homogeneous and space-filling—suited to nutrient exchange (Lorthois and Cassot, 2010). Cortical penetrating arterioles and venules have a

Strahler branching order from 3 to 5 between surface pial vessels and the capillary network (Cassot *et al.*, 2010). Unlike capillaries of the inner retina, it seems there are no boundaries between capillaries arising from different arterioles.

Average total vascular density in temporal cortex is ~ 500 mm/mm³, of which capillaries contribute $\sim 50\%$ (Cassot *et al.*, 2006). This is consistent with human visual cortex, which has an average capillary density of ~ 250 mm/mm³ (Bell and Ball, 1985). Narrow artero-venous anastomoses may exist at the capillary junction, but it is difficult to distinguish these from larger capillaries (Duvernoy *et al.*, 1981).

Ascending cortical venules have $\sim 50\%$ more branches than arterioles; mean branching angle is 118 to 129° (Cassot *et al.*, 2010). Ascending veins include principal veins (Group V5), which arise from subcortical white matter, and are 120–125 μ m wide. The diameter of venules decreases as vessel origin becomes more superficial, ranging from 65 μ m (Group V4) to 20 μ m (Group VI) (Duvernoy *et al.*, 1981). Once ascending venules reach the cortical surface they make a 90° turn to converge on surface venules (~ 130 μ m wide). The surface venous network is anastomotic with channels up to 180 μ m wide, but has fewer anastomoses than the arteriolar network, and some lobules have no surface venous anastomoses. This drains into larger veins adherent to the arachnoid dura (Duvernoy *et al.*, 1981). The largest veins (1.3 to 3.3 mm) cross the subdural space to meet sinuses incorporated into the dura mater (Oka *et al.*, 1985). There are no venous anastomoses in the cerebral grey matter, and only rare reports of arteriovenous anastomoses (Duvernoy *et al.*, 1981).

Occlusion of cortical vessels

The absence of anastomoses between penetrating vessels means that penetrating cortical arterioles and ascending venules represent a physiological bottleneck. Experimental occlusion of penetrating arterioles in rat cortex leads to severe reduction in blood flow velocity in vessels at least seven branches downstream from the occlusion (Nishimura *et al.*, 2010).

In the rat, ascending venules are twice as prevalent as penetrating arterioles, and this is likely to explain the relatively low extent of flow disruption after ascending venule occlusion (Nguyen *et al.*, 2011). In contrast human grey matter penetrating arterioles outnumber venules on average by 2:1 (Cassot *et al.*, 2010), and principal veins are sometimes surrounded by several rings of arterioles. The tissue volume of such vascular units is variable (Duvernoy *et al.*, 1981). The general implication is that, as in the basal ganglia, a low ratio of venules to arterioles in human cortex may mean venous congestion in cerebral malaria disrupts flow to disproportionately large areas of tissue.

Vascular anatomy of the cerebral white matter

The cerebral white matter is supplied by penetrating arterioles from the pial arteriolar network, which remain unbranched within the cerebral grey matter until its deepest layer. These arterioles enter the subcortical white matter perpendicular to the brain surface. Vessels express branches at $\sim 90^\circ$ from the main

trunk—five to ten, depending on trunk length. Only a proportion of arterioles reach the periventricular zone, where they arborize. A few form arteriolar anastomoses (Nonaka *et al.*, 2003a,b). Penetrating arterioles have an internal diameter of 30 to 40 μ m in subcortical white matter, compared to 40 to 60 μ m in the grey matter (Nonaka *et al.*, 2003a), and 100 to 170 μ m in deep white matter (Nonaka *et al.*, 2003b).

There has been disagreement about whether the deep white matter also receives arterioles from ventricular sources (Van den Bergh and Vander Eecken, 1968). Moody *et al.* (1990), Nelson *et al.* (1991) and Nonaka *et al.* (2003b) found no evidence of periventricular arterioles directed towards the brain surface.

Cerebral white matter is drained by superficial medullary veins and deep medullary veins. The former drain subcortical white matter into superficial cerebral veins on the brain surface, and the latter drain periventricular white matter into subependymal veins at the lateral ventricle (Hassler, 1966; Meder *et al.*, 1994; Andeweg, 1996; Nonaka *et al.*, 2003b). Superficial medullary veins are thought to drain the external 1–2 cm of white matter (Meder *et al.*, 1994), and the deep medullary veins the remainder (Hassler, 1966; Hooshmand *et al.*, 1974). Trans-cerebral veins connecting superficial and deep venous systems have been reported (Huang and Wolf, 1964; Hassler, 1966; Meder *et al.*, 1994; Nakamura *et al.*, 1994; Schaller, 2004), but may be artefactual as functional anastomoses between superficial and deep venous systems are not consistent with patterns of injury seen after deep venous system obstruction (Hassler, 1966; Andeweg, 1999). The predominance of haemorrhages in white matter is consistent with relatively long venous drainage pathways (Spitz, 1946).

Cerebral blood flow and metabolism

Like the retina the brain is highly metabolically active (reviewed in Wong-Riley, 2010), and depends on a constant supply of oxygen and glucose (Mckenna *et al.*, 2006).

Normal cerebral blood flow characteristics vary with age and between brain regions (Kety, 1950; Ide and Secher, 2000). Abnormal cerebral blood flow in the middle cerebral arteries has been reported in cases of paediatric cerebral malaria with seizure or raised intracranial pressure (Newton *et al.*, 1996).

Total cerebral blood flow and metabolism changes dramatically during childhood (Kety, 1956; Kennedy and Sokoloff, 1957; Kinnala *et al.*, 1996; Takahashi *et al.*, 1999; Wintermark *et al.*, 2004; Mckenna *et al.*, 2006). Cerebral blood flow increases rapidly during the first year of life (Varela *et al.*, 2012) and flow volume peaks at 55% cardiac output between age 2 to 4 (~ 130 ml/100 g/min) before declining to adult values (Wintermark *et al.*, 2004). In comparison the brain of a resting adult receives $\sim 16.5\%$ cardiac output (Kety, 1950), or ~ 50 ml/100 g/min (Kety and Schmidt, 1948; Madsen *et al.*, 1993; Sokoloff, 2003).

Cerebral metabolic rate for oxygen is also highest from 3 to 6 years, ranging from 4.3 to 6.2 ml O₂/100 g/min (Kennedy and Sokoloff, 1957). The average of 5.25 ml would be $>50\%$ total body oxygen (Mckenna *et al.*, 2006). Adult resting cerebral metabolic rate for O₂ is ~ 3 ml/100 g/min (Kety and Schmidt, 1948; Madsen *et al.*, 1993; Sokoloff, 2003), and accounts for $\sim 20\%$ of total body oxygen consumption (Kety, 1950). Cerebral

arteriovenous oxygen difference is ~40% in adults (Seifert and Secher, 2011), comparable to retinal oxygen extraction of ~50% (McLeod, 2010). The developmental curve for cerebral metabolic rate for glucose follows a similar trajectory to cerebral blood flow, though with a more gradual decline to adult values at around age 17 (Chugani *et al.*, 1987; Kinnala *et al.*, 1996; Chugani, 1998).

The highest regional peak in cerebral blood flow is in the calcarine cortex (area V1, 155 ml/100 g/min, 29 months). Basal ganglia, temporal, frontal, and occipital cortices have lower peaks (~125 to 140 ml/100 g/min) (Wintermark *et al.*, 2004). The highest regional peak in the cerebral metabolic rate for glucose at this age is in the calcarine cortex, transverse temporal cortex, and lenticular nuclei (all >30 μ mol/100 g/min between 1 and 2 years) (Chugani *et al.*, 1987).

Flow in cerebral microvessels

Data on capillary flow dynamics in human brain are scarce, although many studies on animal models exist (Hudetz *et al.*, 1996; Vovenko, 1999; Jespersen and Ostergaard, 2011). Capillary flow velocity is between 0.6 and 2.4 mm/s in rat cortex (Hudetz *et al.*, 1996), which overlaps the lower range of velocities in human perifoveal vessels (Pournaras *et al.*, 2008).

Guibert *et al.* (2010) have modelled blood flow in primate cortex, which has a ratio of arterioles to venules similar to human brain. They found that local haematocrit could vary by approximately a factor of two owing to phase separation. Brain haematocrit measured by dual tracer single-photon emission computed tomography in adult humans is ~76% systemic haematocrit (Sakai *et al.*, 1985). Blood is thought to make up ~3–5% of brain volume, and three quarters of this is venous (An and Lin, 2002). Blood volume is greater in grey (~5 ml/100 g) than white matter (~2 ml/100 g) (Kuppusamy *et al.*, 1996) consistent with greater capillary density in grey matter.

Retina and brain compared: implications for studying neurovascular pathogenesis

Retina and brain microvasculature have much in common, including circulation-tissue barriers and local control over blood flow (Patton *et al.*, 2005). After reviewing microvascular haemorrhology and the microvasculature of retina and brain regions, it seems that sequestration-induced injury could be influenced by several characteristics (Table 2).

Vessel branching

Retinal vessels are relatively long and straight, with right-angled or dichotomous branches. This is also true of cerebral grey matter, white matter and basal ganglia—although brain-specific features are also present. Haemodynamic models suggest near 90° arteriolar branching produces significant variation in haematocrit and viscosity (Ganesan *et al.*, 2010; Guibert *et al.*, 2010) and therefore may be important in

distributing parasitized erythrocytes and fostering sequestration. Right-angled venular confluences may also provide opportunities for sequestration since cells may continue to roll along the endothelium when moving from a smaller to larger vessel before joining the axial flow stream, potentially stripping the endothelial surface layer and exposing ICAM1 (Schmid-Schönbein, 1999; Popel and Johnson, 2005). Local variation in haematocrit and viscosity associated with branching architecture may explain why retinal vessels full of parasitized erythrocytes can be found immediately adjacent to vessels unaffected by sequestration (Lewallen *et al.*, 2000).

Arteriole to venule ratio

Both basal ganglia and cerebral grey matter have more arterioles than venules, whereas in the retina, arterioles and venules are paired. A high ratio of arterioles to venules in the absence of anastomoses may make these brain regions more vulnerable than the retina to the effects of post-capillary venous congestion with parasitized erythrocytes.

Venous drainage and watershed regions

Retina and brain both have vascular watersheds that are amenable to imaging. Although retinal arterial and venous watersheds are identical, retinal arterioles and venules can be distinguished using fluorescein angiogram. In the brain, arterial supply and venous drainage occur over different territories, and radiological changes to these anatomical regions can be assessed using MRI. Retinal capillary non-perfusion is most common in watershed regions, and brain lesions may also follow patterns of venous drainage into superficial and deep systems, especially those of the cerebral white matter (Meder *et al.*, 1994; Andeweg, 1996). Sequestration is thought to mainly involve capillaries and post-capillary venules, and retinal white-centred haemorrhages occur in other conditions involving venous congestion (Duane *et al.*, 1980). These points suggest comparison of retinal and cerebral venous watersheds in cerebral malaria is reasonable, and perhaps that the severity of non-perfusion in retinal watersheds might reflect the degree of T₂ or diffusion-weighted imaging abnormalities in the cerebral white matter in acute cerebral malaria (Fig. 4). The consequences of venous congestion are much greater in brain than retina. For example, swelling of the splenium, or posterior cerebrum (Potchen *et al.*, 2012) could compress the vein of Galen against the tentorium, potentially obstructing outflow from the deep venous system and rapidly raising intracranial pressure (Andeweg, 1999).

Blood flow and metabolism

Adult inner retinal blood flow is roughly half that of the brain. To our knowledge there are no data available on developmental changes to retinal blood flow during childhood. However, cerebral blood flow varies dramatically during childhood development, peaking within the age range typically admitted with paediatric cerebral malaria in high transmission areas (Snow *et al.*, 1997; Wintermark *et al.*, 2004). The median age at admission with cerebral malaria in high transmission areas appears to coincide with the childhood peak in total cerebral blood flow and metabolism. For example, the mean

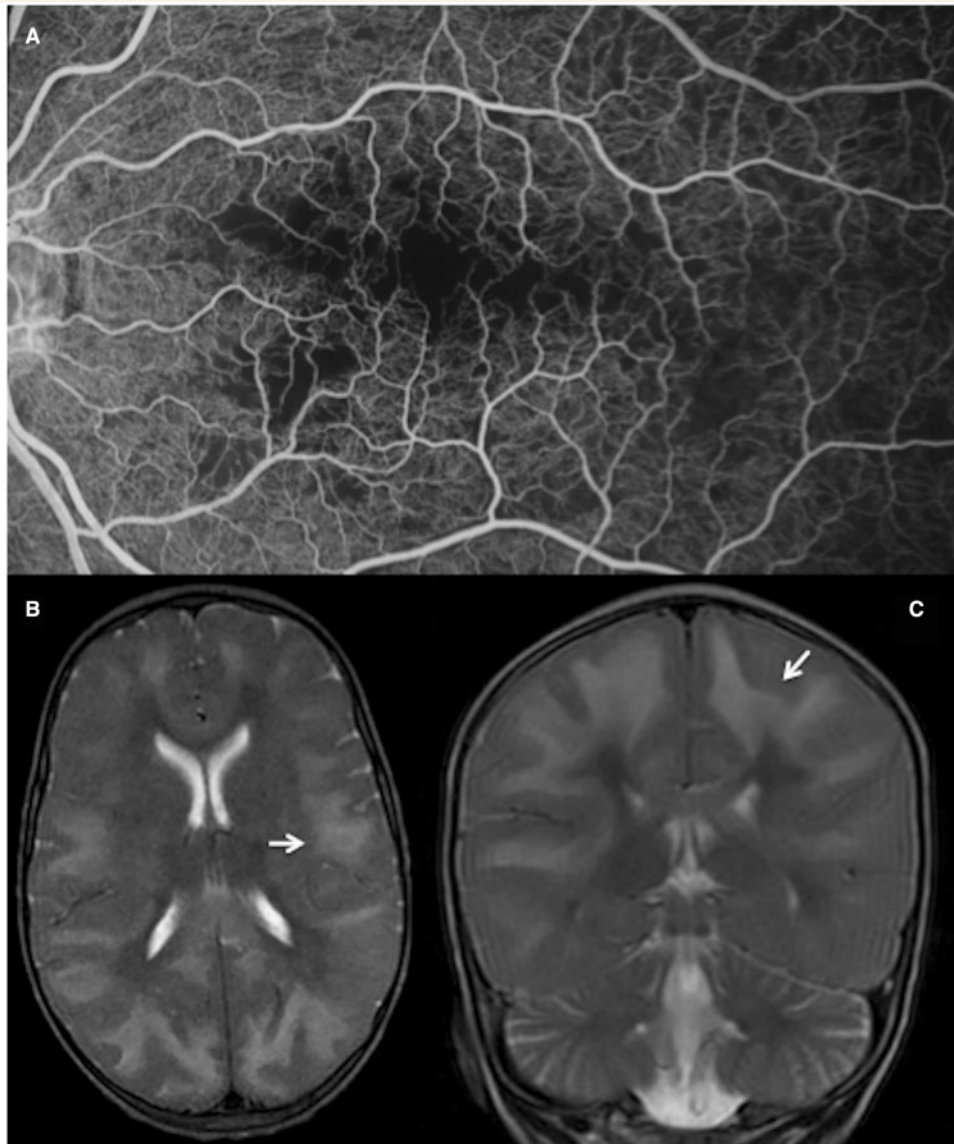


Figure 4 Comparison of retinal and cerebral venous watershed regions. (A) Fluorescein angiogram showing capillary non-perfusion at the macula and horizontal raphe, which is an arteriolar and venular watershed between the supero-temporal and infero-temporal arcades. Axial (B) and coronal (C) MRI images show extensive high T₂ signal in the subcortical white matter of a different child with cerebral malaria (white arrows). The cerebral white matter is the site of a venous watershed between superficial and deep venous systems.

age of children admitted to the paediatric research ward in Blantyre, Malawi, ranged from ~3 to 4 years between 2001–10 (Roca-Feltrer *et al.*, 2012). Snow *et al.* (1997) found the median (IQR) age at admission with cerebral malaria was low in high transmission areas and increased with falling endemicity—ranging from 2 (1.5–6.5) years (hyperholoendemic), 4 (3–5) (mesoendemic), to 6.5 (4–7) years (hypoendemic). A similar pattern is found using residential altitude as a proxy for transmission intensity (Reyburn *et al.*, 2005). As suggested by others (Billig *et al.*, 2012) high metabolic demands may make the paediatric brain more vulnerable to the effects of sequestration than other paediatric organs, and in the context of high transmission predispose to early cerebral complications rather than the acute renal failure or pulmonary oedema seen in adults (Thanachartwet *et al.*, 2013).

Retina and brain are comparable in that they both have very high metabolic demands, and in early childhood the brain may be more susceptible than the retina (and other organs) to the effects of dysfunctional microvascular flow. However cerebral malaria is only one manifestation of severe malaria in children, and it is not clear how high paediatric cerebral metabolic rate for O₂ in isolation could influence which children develop cerebral malaria, and which develop severe malarial anaemia or metabolic acidosis.

Complicating factors

The clinical picture of paediatric cerebral malaria is complicated by the presence of multiple interrelated insults in addition to sequestration, including anaemia, hypoglycaemia, and metabolic acidosis

(WHO, 2000). HIV is known to upregulate ICAM1 (Stins *et al.*, 2003) and infection may complicate cerebral malaria pathogenesis (reviewed in Hochman and Kim, 2012). In addition to systemic insults, seizures are common (Birbeck *et al.*, 2010) and could inflict brain injury without corresponding damage to the retina. Retinal signs could indicate a high tide mark of tissue injury common to particular regions of both retina and brain, which may or may not reach a threshold needed to induce coma, and thereafter trigger additional brain damage from other mechanisms, such as seizure. Alternatively, one or more co-insults may be necessary for development of the cerebral malaria phenotype, as malarial retinopathy is also seen in children with severe malarial anaemia without coma, albeit much less severely (Beare *et al.*, 2004).

Conclusions

Description of the whole brain in terms of greater or lesser similarity to the whole retina is difficult, and probably inappropriate. Rather, analysis of data from retina and brain should take account of anatomical variation within both organs, as neither retina nor brain are homogeneous units. Both have regions where microvasculature may, or may not, be comparable in specific respects that are relevant to a given neurovascular disease.

Retina and brain are similar in ways relevant to paediatric cerebral malaria. Similar vascular pathology suggests both organs experience similar disease processes. Similarities in terms of vessel network architecture, imaging abnormalities in venous watersheds, and high metabolic demand suggest that both organs may be vulnerable to sequestration for the same reasons. These factors may influence delivery of parasitized erythrocytes, the flow conditions necessary for sequestration, and the vulnerability of tissue to ischaemia associated with venous congestion or occlusion. If so, the impact of congestion on common venous anatomy may explain the distribution of MRI brain and retinal fluorescein angiogram lesions in paediatric cerebral malaria.

The retina and brain also have differences. Arteriovenous ratios vary between brain regions, while in the retina arterioles and venules are paired. Cerebral arterial and venous watersheds are different, while retinal watersheds overlap. The paediatric brain has a metabolic peak in early childhood, which is likely to raise cerebral metabolic demands significantly above retinal demands in the age range typically affected by cerebral malaria.

Considering these similarities and differences, a biologically plausible analogy can be made between the retinal periphery, or horizontal raphe, and the cerebral white matter, because these regions have similar vascular architecture. All receive blood from long vessels with near 90° branches, and so may contain blood with disproportionately high microvascular haematocrit and viscosity. The presence of venous watersheds gives little option for collateral drainage from these areas in the event of venous congestion. Given this background, similar degrees of coexistent injury to these retinal and brain areas in a population of children with retinopathy-positive cerebral malaria would suggest that retinal capillary non-perfusion and leakage could be surrogates for brain ischaemia and swelling, and might provide a useful tool to understand cerebral vascular pathogenesis.

Our review has limitations. Only three brain regions are compared with the retina, and comparable data are not available for all geometrical or topological variables at each site. We have resorted to measurements from adults where paediatric data are not available, and we have not attempted comparison of retinal or cerebral microvascular architecture with other organs in which sequestration is minimal or absent. We have not compared paediatric and adult malarial retinopathy—this deserves a separate review.

We have identified significant similarities and differences in retinal and cerebrovascular architecture, blood flow and metabolic demand. These comparisons inform new interpretations of retinal and cerebral data in retinopathy-positive paediatric cerebral malaria by incorporating information on haemorheology and vascular architecture from multiple regions of the CNS. Increasingly comprehensive comparisons of human neurovasculature will provide greater insights into how far retinal vessel changes reflect neurovascular pathology. Mapping the contours of warranted analogy between retina and brain has the potential to strengthen the biological rationale of retinal imaging in neurology, inform interpretation of neurovascular data, and stimulate further hypotheses—for retinopathy-positive paediatric cerebral malaria in particular, and for neurovascular disease in general.

Acknowledgements

Thanks to Dr Vittoria Lutje for help searching for relevant literature, and special thanks to Dr Karl Seydel for many stimulating conversations about malaria over the last 2 years.

Funding

This work was supported by The Wellcome Trust [Grant number 092668/Z/10/Z, Core grant number 084679/Z/08/Z].

References

- Abu Sayeed A, Maude RJ, Hasan MU, Mohammed N, Hoque MG, Dondorp AM, *et al.* Malarial retinopathy in Bangladeshi adults. *Am J Trop Med Hyg* 2011; 84: 141–7.
- Agrawal A, McKibbin MA. Purtscher's and Purtscher-like retinopathies: a review [Review]. *Surv Ophthalmol* 2006; 51: 129–36.
- Akima M. A morphological study on the microcirculation of the central nervous system. Selective vulnerability to hypoxia. *Neuropathology* 1993; 13: 99–112.
- Alm A, Bill A. Ocular and optic nerve blood flow at normal and increased intraocular pressures in monkeys (*Macaca irus*): a study with radioactively labelled microspheres including flow determinations in brain and some other tissues. *Exp Eye Res* 1973; 15: 15–29.
- An H, Lin W. Cerebral venous and arterial blood volumes can be estimated separately in humans using magnetic resonance imaging. *Magn Reson Med* 2002; 48: 583–8.
- Anand-Apte B, Hollyfield JG. Developmental Anatomy of the Retinal and Choroidal Vasculature. In: Dartt DA, editor. *Encyclopedia of the eye*. Oxford: Academic Press 2010.
- Anderson B, Saltzman HA. Retinal oxygen utilization measured by hyperbaric blackout. *Arch Ophthalmol* 1964; 72: 792–5.

- Andeweg J. The anatomy of collateral venous flow from the brain and its value in aetiological interpretation of intracranial pathology [Review]. *Neuroradiology* 1996; 38: 621–628.
- Andeweg J. Consequences of the anatomy of deep venous outflow from the brain [Review]. *Neuroradiology* 1999; 41: 233–41.
- Armah H, Dodoo AK, Wiredu EK, Stiles JK, Adjei AA, Gyasi RK, et al. High-level cerebellar expression of cytokines and adhesion molecules in fatal, paediatric, cerebral malaria. *Ann Trop Med Parasitol* 2005; 99: 629–47.
- Baskurt OK, Meiselman HJ. Blood rheology and hemodynamics [Review]. *Semin thromb hemost* 2003; 29: 435–50.
- Beare NA, Southern C, Chalira C, Taylor TE, Molyneux ME, Harding SP. Prognostic significance and course of retinopathy in children with severe malaria. *Arch Ophthalmol* 2004; 122: 1141–7.
- Beare NA, Glover SJ, Lewallen S, Taylor TE, Harding SP, Molyneux ME. Prevalence of raised intracranial pressure in cerebral malaria detected by optic nerve sheath ultrasound. *Am J Trop Med Hyg* 2012; 87: 985–8.
- Beare NA, Harding SP, Taylor TE, Lewallen S, Molyneux ME. Perfusion abnormalities in children with cerebral malaria and malarial retinopathy. *J Infect Dis* 2009; 199: 263–271.
- Beare NA, Lewallen S, Taylor TE, Molyneux ME. Redefining cerebral malaria by including malaria retinopathy. *Future Microbiol* 2011; 6: 349–55.
- Bek T, Jensen PK. Three-dimensional structure of human retinal vessels studied by vascular casting. *Acta Ophthalmol (Copenh)* 1993; 71: 506–13.
- Bell MA, Ball MJ. Laminar variation in the microvascular architecture of normal human visual cortex (area 17). *Brain Res* 1985; 335: 139–43.
- Van den Bergh R, Van der Eecken H. Anatomy and embryology of cerebral circulation. *Prog Brain Res* 1968; 30: 1–25.
- Berntson GM. The characterization of topology: a comparison of four topological indices for rooted binary trees. *J Theor Biol* 1995; 177: 271–81.
- Billig EMW, O'Meara WP, Riley EM, McKenzie FE. Developmental allometry and paediatric malaria. *Malar J* 2012; 11: 64.
- Birbeck GL, Molyneux ME, Kaplan PW, Seydel KB, Chimalizeni YF, Kawaza K, et al. Blantyre Malaria Project Epilepsy Study (BMPEs) of neurological outcomes in retinopathy-positive paediatric cerebral malaria survivors: a prospective cohort study. *Lancet* 2010; 9: 1173–81.
- Biról G, Wang S, Budzynski E, Wangsa-Wirawan ND, Linsenmeier RA. Oxygen distribution and consumption in the macaque retina. *Am J Physiol Heart Circ Physiol* 2007; 293: H1696–704.
- Bronzan RN, Taylor TE, Mwenechanya J, Tembo M, Kayira K, Bwanaisa L, et al. Bacteremia in Malawian children with severe malaria: prevalence, etiology, HIV coinfection, and outcome. *J Infect Dis* 2007; 195: 895–904.
- Brown H, Rogerson S, Taylor T, Tembo M, Mwenechanya J, Molyneux M, et al. Blood-brain barrier function in cerebral malaria in Malawian children. *Am J Trop Med Hyg* 2001; 64: 207–13.
- Browning DJ. Patchy ischemic retinal whitening. *Ophthalmology* 2004; 111: 606–7.
- Burton K, Nyong O, John W, Inkoom E, Pinder M, Bailey R. Retinopathy in Gambian children admitted to hospital with malaria. *Trop Doct* 2004; 34: 1–4.
- Cassot F, Lauwers F, Fouard C, Prohaska S, Lauwers-Cances V. A novel three-dimensional computer-assisted method for a quantitative study of microvascular networks of the human cerebral cortex. *Microcirculation* 2006; 13: 1–18.
- Cassot F, Lauwers F, Lorthois S, Puwanarajah P, Cances-Lauwers V, Duvernoy H. Branching patterns for arterioles and venules of the human cerebral cortex. *Brain Res* 2010; 1313: 62–78.
- Cheung N, Islam FMA, Saw Seang M, Shankar A, De Haseth K, Mitchell P, et al. Distribution and associations of retinal vascular caliber with ethnicity, gender, and birth parameters in young children. *Invest Ophthalmol Vis Sci* 2007; 48: 1018–24.
- Cho YI, Cho DJ. Hemorheology and microvascular disorders [Review]. *Korean Circ J* 2011; 41: 287–95.
- Chotivanich K, Sritabal J, Udomsangpetch R, Newton P, Stepniewska KA, Ruangveerayuth R, et al. Platelet-induced autoagglutination of Plasmodium falciparum-infected red blood cells and disease severity in Thailand. *J Infect Dis* 2004; 189: 1052–5.
- Chugani HT. A critical period of brain development: studies of cerebral glucose utilization with PET. *Prev Med* 1998; 27: 184–8.
- Chugani HT, Phelps ME, Mazziotta JC. Positron emission tomography study of human brain functional development. *Ann Neurol* 1987; 22: 487–97.
- Cogan DG, Kuwabara T. Comparison of retinal and cerebral vasculature in trypsin digest preparations. *Br J Ophthalmol* 1984; 68: 10–12.
- Craig A, Scherf A. Molecules on the surface of the Plasmodium falciparum infected erythrocyte and their role in malaria pathogenesis and immune evasion [Review]. *Mol Biochem Parasitol* 2001; 115: 129–43.
- Crane JJ, Liversidge J. Mechanisms of leukocyte migration across the blood-retina barrier [Review]. *Semin Immunopathol* 2008; 30: 165–77.
- Dondorp AM, Angus BJ, Hardeman MR, Chotivanich KT, Silamut K, Ruangveerayuth R, et al. Prognostic significance of reduced red blood cell deformability in severe falciparum malaria. *Am J Trop Med Hyg* 1997; 57: 507–11.
- Dondorp AM, Omodeo-Salè F, Chotivanich K, Taramelli D, White NJ. Oxidative stress and rheology in severe malaria [Review]. *Redox Rep* 2003; 8: 292–4.
- Dondorp AM, Lee SJ, Faiz MA, Mishra S, Price R, Tjitra E, et al. The relationship between age and the manifestations of and mortality associated with severe malaria. *Clin Infect Dis* 2008; 47: 151–7.
- Dorner GT, Polska E, Garhöfer G, Zawinka C, Frank B, Schmetterer L. Calculation of the diameter of the central retinal artery from noninvasive measurements in humans. *Curr Eye Res* 2002; 25: 341–5.
- Dorovini-Zis K, Schmidt K, Huynh H, Fu W, Whitten Richard O, Milner D, et al. The neuropathology of fatal cerebral malaria in malawian children. *Am J Pathol* 2011; 178: 2146–58.
- Doubal FN, Hokke PE, Wardlaw JM. Retinal microvascular abnormalities and stroke: a systematic review [Review]. *J Neurol Neurosurg Psychiatry* 2009; 80: 158–65.
- Doubal FN, MacGillivray TJ, Patton N, Dhillon B, Dennis MS, Wardlaw JM. Fractal analysis of retinal vessels suggests that a distinct vasculopathy causes lacunar stroke. *Neurology* 2010; 74: 1102–7.
- Duane TD, Osher RH, Green WR. White centered hemorrhages: their significance. *Ophthalmology* 1980; 87: 66–9.
- Duguid IG, Boyd AW, Mandel TE. Adhesion molecules are expressed in the human retina and choroid. *Curr Eye Res* 1992; 11 (Suppl): 153–9.
- Duvernoy HM, Delon S, Vannson JL. Cortical blood vessels of the human brain. *Brain Res Bull* 1981; 7: 519–79.
- Faraci FM. Protecting against vascular disease in brain [Review]. *Am J Physiol Heart Circ Physiol* 2011; 300: H1566–82.
- Fedosov DA, Caswell B, Karniadakis GE. Wall shear stress-based model for adhesive dynamics of red blood cells in malaria. *Biophys J* 2011a; 100: 2084–93.
- Fedosov DA, Caswell B, Suresh S, Karniadakis GE. Quantifying the biophysical characteristics of Plasmodium-falciparum-parasitized red blood cells in microcirculation. *Proc Natl Acad Sci USA* 2011b; 108: 35–9.
- Feke GT, Tagawa H, Deupree DM, Goger DG, Sebag J, Weiter JJ. Blood flow in the normal human retina. *Invest Ophthalmol Vis Sci* 1989; 30: 58–65.
- Funatsu H, Yamashita H, Sakata K, Noma H, Mimura T, Suzuki M, et al. Vitreous levels of vascular endothelial growth factor and intercellular adhesion molecule 1 are related to diabetic macular edema. *Ophthalmology* 2005; 112: 806–16.
- Ganesan P, He S, Xu H. Analysis of retinal circulation using an image-based network model of retinal vasculature. *Microvasc Res* 2010; 80: 99–109.
- Geeraerts T, Devys J-M, Berges O, Dureau P, Plaud B. Sevoflurane effects on retrobulbar arteries blood flow in children. *Br J Anaesth* 2005; 94: 636–41.

- Griffiths MJ, Ndungu F, Baird KL, Muller DP, Marsh K, Newton CR. Oxidative stress and erythrocyte damage in Kenyan children with severe *Plasmodium falciparum* malaria. *Br J Haematol* 2001; 113: 486–91.
- Guibert R, Fonta C, Plouraboué F. Cerebral blood flow modeling in primate cortex. *J Cereb Blood Flow Metab* 2010; 30: 1860–73.
- Harding SP, Lewallen S, Beare NA, Smith A, Taylor TE, Molyneux ME. Classifying and grading retinal signs in severe malaria [Review]. *Trop Doct* 2006; 36 (Suppl 1): 1–13.
- Hassler O. Deep cerebral venous system in man. A microangiographic study on its areas of drainage and its anastomoses with the superficial cerebral veins. *Neurology* 1966; 16: 505–11.
- Hayreh SS. *In vivo* choroidal circulation and its watershed zones [Review]. *Eye (Lond)* 1990; 4: 273–89.
- Hayreh SS. Physiological anatomy of the retinal vasculature. In: Dartt DA, editor. *Encyclopedia of the eye*. Elsevier; 2010a. p. 431–8.
- Hayreh SS. Physiological anatomy of the choroidal vasculature. In: Dartt DA, editor. *Encyclopedia of the Eye*. Elsevier; 2010b. p. 418–430.
- Hero M, Harding SP, Riva CE, Winstanley PA, Peshu N, Marsh K. Photographic and angiographic characterization of the retina of Kenyan children with severe malaria. *Arch Ophthalmol* 1997; 115: 997–1003.
- Van der Heyde HC, Nolan J, Combes V, Gramaglia I, Grau GE. A unified hypothesis for the genesis of cerebral malaria: sequestration, inflammation and hemostasis leading to microcirculatory dysfunction [Review]. *Trends Parasitol* 2006; 22: 503–8.
- Hirsch S, Reichold J, Schneider M, Székely G, Weber B. Topology and hemodynamics of the cortical cerebrovascular system [Review]. *J Cereb Blood Flow Metab* 2012; 32: 952–67.
- Hochman S, Kim K. The impact of HIV coinfection on cerebral malaria pathogenesis [Review]. *J Neuroparasitology* 2012; 3: 1–29.
- Hooshmand I, Rosenbaum AE, Stein RL. Radiographic anatomy of normal cerebral deep medullary veins: criteria for distinguishing them from their abnormal counterparts. *Neuroradiology* 1974; 7: 75–84.
- Huang YP, Wolf BS. Veins of the white matter of the cerebral hemispheres (the medullary veins). *Am J Roentgenol Radium Ther Nucl Med* 1964; 92: 739–55.
- Hudetz AG, Fehér G, Kampine JP. Heterogeneous autoregulation of cerebrocortical capillary flow: evidence for functional thoroughfare channels? *Microvasc Res* 1996; 51: 131–6.
- Hughes AD, Wong Tien Y, Witt N, Evans R, Thom SA, Klein BE, et al. Determinants of retinal microvascular architecture in normal subjects. *Microcirculation* 2009; 16: 159–66.
- Ide K, Secher NH. Cerebral blood flow and metabolism during exercise [Review]. *Prog Neurobiol* 2000; 61: 397–414.
- Idro R, Jenkins NE, Newton CRJ. Pathogenesis, clinical features, and neurological outcome of cerebral malaria [Review]. *Lancet Neurol* 2005; 4: 827–40.
- International Conference on Harmonisation. ICH Topic E9 Statistical Principles for Clinical Trials. 1998. URL: <http://www.ich.org/products/guidelines/efficacy/efficacy-single/article/statistical-principles-for-clinical-trials.html> [29 May 2013 date last accessed].
- Jespersen SN, Ostergaard L. The roles of cerebral blood flow, capillary transit time heterogeneity, and oxygen tension in brain oxygenation and metabolism. *J Cereb Blood Flow Metab* 2011; 32: 264–77.
- Jonas JB, Schneider U, Naumann GO. Count and density of human retinal photoreceptors. *Graefes Arch Clin Exp Ophthalmol* 1992; 230: 505–10.
- Kaul D. K, Roth EF, Nagel RL, Howard RJ, Handunnetti SM. Rosetting of *Plasmodium falciparum*-infected red blood cells with uninfected red blood cells enhances microvascular obstruction under flow conditions. *Blood* 1991; 78: 812–9.
- Kennedy C, Sokoloff L. An adaptation of the nitrous oxide method to the study of the cerebral circulation in children; normal values for cerebral blood flow and cerebral metabolic rate in childhood. *J Clin Invest* 1957; 36: 1130–7.
- Kety SS. Blood flow and metabolism of the human brain in health and disease. *Trans Stud Coll Physicians Phila* 1950; 18: 103–8.
- Kety SS. Human cerebral blood flow and oxygen consumption as related to aging. *J Chronic Dis* 1956; 3: 478–86.
- Kety SS, Schmidt CF. The nitrous oxide method for the quantitative determination of cerebral blood flow in man: theory, procedure and normal values. *J Clin Invest* 1948; 27: 476–83.
- Kinnala A, Suhonen-Polvi H, Aärimaa T, Kero P, Korvenranta H, Ruotsalainen U, et al. Cerebral metabolic rate for glucose during the first six months of life: an FDG positron emission tomography study. *Arch Dis Child Fetal Neonatal Ed* 1996; 74: F153–7.
- Kuppusamy K, Lin W, Cizek GR, Haacke EM. *In vivo* regional cerebral blood volume: quantitative assessment with 3D T1-weighted pre- and postcontrast MR imaging. *Radiology* 1996; 201: 106–12.
- Kur J, Newman E a, Chan-Ling T. Cellular and physiological mechanisms underlying blood flow regulation in the Retina and Choroid in health and disease [Review]. *Prog Retin Eye Res* 2012; 31: 377–406.
- Kuwabara T, Cogan DG. Studies of retinal vascular patterns. I. Normal architecture. *Arch Ophthalmol* 1960; 64: 904–11.
- Lauwers F, Cassot F, Lauwers-Cances V, Puwanarajah P, Duvernoy H. Morphometry of the human cerebral cortex microcirculation: general characteristics and space-related profiles. *Neuroimage* 2008; 39: 936–48.
- Lee KE, Klein BEK, Klein R, Knudtson MD. Familial aggregation of retinal vessel caliber in the beaver dam eye study. *Invest Ophthalmol Vis Sci* 2004; 45: 3929–33.
- Lewallen S, Harding SP, Ajewole J, Schulenburg WE, Molyneux ME, Marsh K, et al. A review of the spectrum of clinical ocular fundus findings in *P. falciparum* malaria in African children with a proposed classification and grading system. *Trans R Soc Trop Med Hyg* 1999; 93: 619–22.
- Lewallen SA, White VA, Whitten RO, Gardiner J, Hoar B, Lindley J, et al. Clinical-histopathological correlation of the abnormal retinal vessels in cerebral malaria. *Arch Ophthalmol* 2000; 118: 924–8.
- Lewallen Susan, Bronzan RN, Beare NA, Harding SP, Molyneux ME, Taylor TE. Using malarial retinopathy to improve the classification of children with cerebral malaria. *Trans R Soc Trop Med Hyg* 2008; 102: 1089–94.
- Li LJ, Cheung CY-L, Liu Y, Chia A, Selvaraj P, Lin X-Y, et al. Influence of blood pressure on retinal vascular caliber in young children. *Ophthalmology* 2011; 118: 1459–65.
- Ling R, James B. White-centred retinal haemorrhages (Roth spots). *Postgrad Med J* 1998; 74: 581–2.
- Lipowsky HH. Microvascular rheology and hemodynamics [Review]. *Microcirculation* 2005; 12: 5–15.
- Lochhead J, Movaffaghly A, Falsini B, Harding S, Riva C, Molyneux M. The effects of hypoxia on the ERG in paediatric cerebral malaria. *Eye* 2010; 24: 259–64.
- Lorthois S, Cassot F. Fractal analysis of vascular networks: insights from morphogenesis. *J Theor Biol* 2010; 262: 614–33.
- Lu M, Perez VL, Ma N, Miyamoto K, Peng HB, Liao JK, et al. VEGF increases retinal vascular ICAM-1 expression *in vivo*. *Invest Ophthalmol Vis Sci* 1999; 40: 1808–12.
- Mackenzie S. Retinal haemorrhages and melanaemia as symptoms of ague. *Medical Times and Gazette*. London, 1877; 23 June: 663–5.
- MacPherson GG, Warrell MJ, White NJ, Loareesuwan S, Warrell DA. Human cerebral malaria. A quantitative ultrastructural analysis of parasitized erythrocyte sequestration. *Am J Pathol* 1985; 119: 385–401.
- Madsen PL, Holm S, Herning M, Lassen NA. Average blood flow and oxygen uptake in the human brain during resting wakefulness: a critical appraisal of the Kety-Schmidt technique. *J Cereb Blood Flow Metab* 1993; 13: 646–55.
- Maude RJ, Beare NAV, Abu Sayeed A, Chang CC, Charunwatthana P, Faiz MA, et al. The spectrum of retinopathy in adults with *Plasmodium falciparum* malaria. *Trans R Soc Trop Med Hyg* 2009; 103: 665–71.
- Mckenna MC, Gruetter R, Sonnewald U, Waagepetersen HS, Schousboe A. Energy metabolism of the brain. In: Seigel GJ,

- Albers RW, Brady ST, Price DL, editors. Basic neurochemistry: molecular, cellular and medical aspects. Amsterdam: Elsevier; 2006. p. 535.
- McLeod D. Krogh cylinders in retinal development, panretinal hypoperfusion and diabetic retinopathy [Review]. *Acta Ophthalmol* 2010; 88: 817–35.
- Medana IM, Day NPJ, Sachanonta N, Mai NT, Dondorp AM, Pongponratn E, et al. Coma in fatal adult human malaria is not caused by cerebral oedema. *Malar J* 2011; 10: 267.
- Meder JF, Chiras J, Roland J, Guinet P, Bracard S, Bargy F. Venous territories of the brain [Review]. *J Neuroradiol* 1994; 21: 118–33.
- Mendis KR, Balaratnasingam C, Yu P, Barry CJ, McAllister IL, Cringle Stephen J, et al. Correlation of histologic and clinical images to determine the diagnostic value of fluorescein angiography for studying retinal capillary detail. *Invest Ophthalmol Vis Sci* 2010; 51: 5864–9.
- Miller LH, Ackerman HC, Su X-Z, Wellems TE. Malaria biology and disease pathogenesis: insights for new treatments [Review]. *Nat Med* 2013; 19: 156–67.
- Miyawaki E, Statland J. Cerebral blood vessels: arteries. In: Aminoff MJ, Daroff RB, editors. *Encyclopedia of the Neurological Sciences*. New York: Academic Press; 2003a. p. 584–591.
- Miyawaki E, Statland J. Cerebral blood vessels: veins and venous sinuses. In: Aminoff MJ, Daroff RB, editors. *Encyclopedia of the Neurological Sciences*. New York: Academic Press; 2003b. p. 591–594.
- Molyneux ME, Taylor TE, Wirima JJ, Borgstein A. Clinical features and prognostic indicators in paediatric cerebral malaria: a study of 131 comatose Malawian children. *Q J Med* 1989; 71: 441–59.
- Montgomery J, Mphande FA, Berriman M, Pain A, Rogerson SJ, Taylor Terrie E, et al. Differential var gene expression in the organs of patients dying of falciparum malaria. *Mol Microbiol* 2007; 65: 959–67.
- Moody DM, Bell MA, Challa VR. Features of the cerebral vascular pattern that predict vulnerability to perfusion or oxygenation deficiency: an anatomic study. *AJNR Am J Neuroradiol* 1990; 11: 431–9.
- Moxon CA, Grau GE, Craig AG. Malaria: modification of the red blood cell and consequences in the human host [Review]. *Br J Haematol* 2011; 154: 670–9.
- Moxon CA, Heyderman RS, Wassmer SC. Dysregulation of coagulation in cerebral malaria [Review]. *Mol Biochem Parasitol* 2009; 166: 99–108.
- Moxon CA, Wassmer SC, Milner DA, Chisala N V, Taylor TE, Seydel KB, et al. Loss of endothelial protein C receptors links coagulation and inflammation to parasite sequestration in cerebral malaria in African children. *Blood* 2013; 22: 842–51.
- Mullins RF, Skeie JM, Malone EA, Kuehn MH. Macular and peripheral distribution of ICAM-1 in the human choriocapillaris and retina. *Mol Vis* 2006; 12: 224–35.
- Nagaoka T, Sato E, Takahashi A, Sogawa K, Yokota H, Yoshida A. Effect of aging on retinal circulation in normotensive healthy subjects. *Exp Eye Res* 2009; 89: 887–91.
- Nagaoka T, Yoshida A. Noninvasive evaluation of wall shear stress on retinal microcirculation in humans. *Invest Ophthalmol Vis Sci* 2006; 47: 1113–9.
- Nagatake T, Hoang VT, Tegoshi T, Rabbage J, Ann TK, Aikawa M. Pathology of falciparum malaria in Vietnam. *Am J Trop Med Hyg* 1992; 47: 259–64.
- Nakamura Y, Okudera T, Hashimoto T. Vascular architecture in white matter of neonates: its relationship to periventricular leukomalacia. *J Neuropathol Exp Neurol* 1994; 53: 582–9.
- Narsaria N, Mohanty C, Das BK, Mishra SP, Prasad R. Oxidative stress in children with severe malaria. *J Trop Pediatr* 2011; 58: 147–50.
- Nelson MD, Gonzalez-Gomez I, Gilles FH. Dyke Award. The search for human telencephalic ventriculofugal arteries. *AJNR Am J Neuroradiol* 1991; 12: 215–22.
- Newton CR, Kirkham FJ, Winstanley PA, Pasvol G, Peshu N, Warrell DA, et al. Intracranial pressure in African children with cerebral malaria. *Lancet* 1991; 337: 573–6.
- Newton CR, Marsh K, Peshu N, Kirkham FJ. Perturbations of cerebral hemodynamics in Kenyans with cerebral malaria. *Pediatr Neurol* 1996; 15: 41–9.
- Newton CR, Peshu N, Kendall B, Kirkham FJ, Sowunmi A, Waruiru C, et al. Brain swelling and ischaemia in Kenyans with cerebral malaria. *Arch Dis Child* 1994; 70: 281–7.
- Newton CR, Taylor TE, Whitten RO. Pathophysiology of fatal falciparum malaria in African children [Review]. *Am J Trop Med Hyg* 1998; 58: 673–83.
- Nguyen J, Nishimura N, Fetcho RN, Iadecola C, Schaffer CB. Occlusion of cortical ascending venules causes blood flow decreases, reversals in flow direction, and vessel dilation in upstream capillaries. *J Cereb Blood Flow Metab* 2011; 1–12.
- Nishimura N, Rosidi NL, Iadecola C, Schaffer CB. Limitations of collateral flow after occlusion of a single cortical penetrating arteriole. *J Cereb Blood Flow Metab* 2010; 30: 1914–27.
- Nonaka H, Akima M, Hatori T, Nagayama T, Zhang Z, Ihara F. The microvasculature of the cerebral white matter: arteries of the subcortical white matter. *J Neuropathol Exp Neurol* 2003a; 62: 154–61.
- Nonaka H, Akima M, Hatori T, Nagayama T, Zhang Z, Ihara F. Microvasculature of the human cerebral white matter: arteries of the deep white matter. *Neuropathology* 2003b; 23: 111–8.
- Nonaka H, Akima M, Nagayama T, Hatori T. The fundamental architecture of the microvasculature of the basal ganglia and changes in senility. *Neuropathology* 1998; 18: 47–54.
- Nowinski WL. Proposition of a new classification of the cerebral veins based on their termination [Review]. *Surg Radiol Anat* 2012; 34: 107–14.
- Oka K, Rhoton AL, Barry M, Rodriguez R. Microsurgical anatomy of the superficial veins of the cerebrum. *Neurosurgery* 1985; 17: 711–48.
- Ono M, Rhoton AL, Peace D, Rodriguez RJ. Microsurgical anatomy of the deep venous system of the brain. *Neurosurgery* 1984; 15: 621–57.
- Oo MM, Aikawa M, Than T, Aye TM, Myint PT, Igarashi I, et al. Human cerebral malaria: a pathological study. *J Neuropathol Exp Neurol* 1987; 46: 223–31.
- Pain A, Ferguson DJ, Kai O, Urban BC, Lowe B, Marsh K, et al. Platelet-mediated clumping of Plasmodium falciparum-infected erythrocytes is a common adhesive phenotype and is associated with severe malaria. *Proc Natl Acad Sci USA* 2001; 98: 1805–10.
- Patton N, Aslam T, Macgillivray T, Pattie A, Deary IJ, Dhillon B. Retinal vascular image analysis as a potential screening tool for cerebrovascular disease: a rationale based on homology between cerebral and retinal microvasculatures [Review]. *J Anat* 2005; 206: 319–48.
- Patton N, Aslam TM, MacGillivray T, Deary IJ, Dhillon B, Eikelboom RH, et al. Retinal image analysis: concepts, applications and potential [Review]. *Prog Ret Eye Res* 2006; 25: 99–127.
- Penman A, Talbot JF, Chuang EL, Bird AC, Serjeant GR. Peripheral retinal vasculature in normal Jamaican children. *Br J Ophthalmol* 1994; 78: 615–7.
- Pongponratn E, Riganti M, Punpoowong B, Aikawa M. Microvascular sequestration of parasitized erythrocytes in human falciparum malaria: a pathological study. *Am J Trop Med Hyg* 1991; 44: 168–75.
- Pongponratn E, Turner GDH, Day NPJ, Phu NH, Simpson JA, Stepniewska K, et al. An ultrastructural study of the brain in fatal Plasmodium falciparum malaria. *Am J Trop Med Hyg* 2003; 69: 345–59.
- Ponsford MJ, Medana IM, Prapansilp P, Hien TT, Lee SJ, Dondorp AM, et al. Sequestration and microvascular congestion are associated with coma in human cerebral malaria. *J Infect Dis* 2012; 205: 663–71.
- Popel AS, Johnson PC. Microcirculation and hemorheology [Review]. *Annu Rev Fluid Mech* 2005; 37: 43–69.
- Potchen MJ, Kampondeni SD, Seydel KB, Birbeck GL, Hammond CA, Bradley WG, et al. Acute brain MRI findings in 120 Malawian children with cerebral malaria: new insights into an ancient disease. *AJNR Am J Neuroradiol* 2012; 33: 1740–6.
- Pournaras CJ, Rungger-Brändle E, Riva Charles E, Hardarson SH, Stefansson E. Regulation of retinal blood flow in health and disease [Review]. *Prog Retin Eye Res* 2008; 27: 284–330.
- Pries AR, Secomb TW, Gaetgens P. The endothelial surface layer [Review]. *Pflugers Arch* 2000; 440: 653–66.

- Rasalkar DD, Paunipagar BK, Sanghvi D, Sonawane BD, Loniker P. Magnetic resonance imaging in cerebral malaria: a report of four cases. *Br J Radiol* 2011; 84: 380–5.
- Reina-de La Torre F, Rodriguez-baeza A, Sahuquillo-Barris J. Morphological characteristics and distribution pattern of the arterial vessels in human cerebral cortex: a scanning electron microscope study. *Anat Rec* 1998; 251: 87–96.
- Reyburn H, Mbatia R, Drakeley C, Bruce J, Carneiro I, Olomi R, et al. Association of transmission intensity and age with clinical manifestations and case fatality of severe *Plasmodium falciparum* malaria. *JAMA* 2005; 293: 1461–70.
- Roca-Feltrre A, Kwizombe CJ, Sanjoaquin MA, Sesay SS, Faragher B, Harrison J, et al. Lack of decline in childhood malaria, Malawi, 2001–2010. *Emerg Infect Dis* 2012; 18: 272–8.
- Rochtchina E, Wang JJ, Taylor B, Wong TY, Mitchell P. Ethnic variability in retinal vessel caliber: a potential source of measurement error from ocular pigmentation? The Sydney Childhood Eye Study. *Invest Ophthalmol Vis Sci* 2008; 49: 1362–6.
- Rowe JA, Claessens A, Corrigan RA, Arman M. Adhesion of *Plasmodium falciparum*-infected erythrocytes to human cells: molecular mechanisms and therapeutic implications. *Expert Rev Mol Med* 2009; 11: e16.
- Sakai F, Nakazawa K, Tazaki Y, Ishii K, Hino H, Igarashi H, et al. Regional cerebral blood volume and hematocrit measured in normal human volunteers by single-photon emission computed tomography. *J Cereb Blood Flow Metab* 1985; 5: 207–13.
- Sarda V, Nakashima K, Wolff B, Sahel JA, Paques M. Topography of patchy retinal whitening during acute perfused retinal vein occlusion by optical coherence tomography and adaptive optics fundus imaging. *Eur J Ophthalmol* 2011; 21: 653–6.
- Sarpeshkar R. Ultra low power bioelectronics: fundamentals, biomedical applications, and bio-inspired systems. Cambridge: Cambridge University press; 2010. p. 748.
- Schaller B. Physiology of cerebral venous blood flow: from experimental data in animals to normal function in humans [Review]. *Brain Res Brain Res Rev* 2004; 46: 243–60.
- Schmid-Schönbein GW. Biomechanics of microcirculatory blood perfusion [Review]. *Annu Rev Biomed Eng* 1999; 1: 73–102.
- Seifert T, Secher NH. Sympathetic influence on cerebral blood flow and metabolism during exercise in humans [Review]. *Prog Neurobiol* 2011; 95: 406–26.
- Sein KK, Maeno Y, Thuc H V, Anh TK, Aikawa M. Differential sequestration of parasitized erythrocytes in the cerebrum and cerebellum in human cerebral malaria. *Am J Trop Med Hyg* 1993; 48: 504–11.
- Semmer AE, McLoon LK, Lee MS. Orbital vascular anatomy. In: Dartt DA, editor. *Encyclopedia of the Eye*. Elsevier; 2010. p. 241–251.
- Silamut K, Phu NH, Whitty C, Turner GD, Louwrier K, Mai NT, et al. A quantitative analysis of the microvascular sequestration of malaria parasites in the human brain. *Am J Pathol* 1999; 155: 395–410.
- Smith JR, Choi D, Chipps TJ, Pan Y, Zamora DO, Davies MH, et al. Unique gene expression profiles of donor-matched human retinal and choroidal vascular endothelial cells. *Invest Ophthalmol Vis Sci* 2007; 48: 2676–84.
- Snow RW, Omumbo JA, Lowe B, Molyneux CS, Obiero JO, Palmer A, et al. Relation between severe malaria morbidity in children and level of *Plasmodium falciparum* transmission in Africa. *Lancet* 1997; 349: 1650–4.
- Sokoloff L. Cerebral metabolism and blood flow. In: Aminoff MJ, Daroff RB, editors. *Encyclopedia of the Neurological Sciences*. New York: Academic Press; 2003. p. 609–617.
- Sperber GO, Bill A. Blood flow and glucose consumption in the optic nerve, retina and brain: effects of high intraocular pressure. *Exp Eye Res* 1985; 41: 639–53.
- Spitz S. The pathology of acute falciparum malaria. *Mil Surg* 1946; 99: 555–72.
- Spitznas M, Bornfeld N. The architecture of the most peripheral retinal vessels. *Albrecht Von Graefes Arch Klin Exp Ophthalmol* 1977; 203: 217–29.
- Stefánsson E, Wilson CA, Lightman SL, Kuwabara T, Palestine AG, Wagner HG. Quantitative measurements of retinal edema by specific gravity determinations. *Invest Ophthalmol Vis Sci* 1987; 28: 1281–9.
- Stins MF, Pearce D, Di Cello F, Erdreich-Epstein A, Pardo CA, Sik Kim K. Induction of intercellular adhesion molecule-1 on human brain endothelial cells by HIV-1 gp120: role of CD4 and chemokine coreceptors. *Lab Invest* 2003; 83: 1787–98.
- Sun C, Ponsonby A, Wong Tien Y, Brown SA, Kearns LS, Cochrane J, et al. Effect of birth parameters on retinal vascular caliber: the Twins Eye Study in Tasmania. *Hypertension* 2009; 53: 487–93.
- Takahashi T, Shirane R, Sato S, Yoshimoto T. Developmental changes of cerebral blood flow and oxygen metabolism in children. *AJNR Am J Neuroradiol* 1999; 20: 917–22.
- Tam J, Martin JA, Roorda A. Noninvasive visualization and analysis of parafoveal capillaries in humans. *Invest Ophthalmol Vis Sci* 2010; 51: 1691–8.
- Tam J, Tiruveedhula P, Roorda A. Characterization of single-file flow through human retinal parafoveal capillaries using an adaptive optics scanning laser ophthalmoscope. *Biomed Opt Express* 2011; 2: 781–93.
- Tapp RJ, Williams C, Witt N, Chaturvedi N, Evans R, Thom SA, et al. Impact of size at birth on the microvasculature: the Avon longitudinal study of parents and children. *Pediatrics* 2007; 120: e1225–8.
- Taylor B, Rochtchina E, Wang JJ, Wong T Y, Heikal S, Saw SM, et al. Body mass index and its effects on retinal vessel diameter in 6-year-old children. *Int J Obes (Lond)* 2007; 31: 1527–33.
- Taylor TE, Fu WJ, Carr RA, Whitten RO, Mueller JS, Fosiko NG, et al. Differentiating the pathologies of cerebral malaria by postmortem parasite counts. *Nat Med* 2004; 10: 143–5.
- Teksam M, Moharir M, Deveber G, Shroff M. Frequency and topographic distribution of brain lesions in pediatric cerebral venous thrombosis. *AJNR Am J Neuroradiol* 2008; 29: 1961–5.
- Thanachartwet V, Desakorn V, Sahassananda D, Kyaw Win KK, Supaporn T. Acute renal failure in patients with severe falciparum malaria: using the WHO 2006 and RIFLE criteria. *Int J Nephrol* 2013; 2013: 841518.
- Turner G. Cerebral malaria [Review]. *Brain Pathol* 1997; 7: 569–82.
- Turner L, Lavstsen T, Berger SS, Wang CW, Petersen JEV, Avril M, et al. Severe malaria is associated with parasite binding to endothelial protein C receptor. *Nature* 2013; 498: 502–5.
- Varela M, Groves AM, Arichi T, Hajnal JV. Mean cerebral blood flow measurements using phase contrast MRI in the first year of life. *NMR Biomed* 2012; 25: 1063–72.
- Vovenko E. Distribution of oxygen tension on the surface of arterioles, capillaries and venules of brain cortex and in tissue in normoxia: an experimental study on rats. *Pflügers Arch* 1999; 437: 617–23.
- Wang Q, Kocaoglu OP, Cense B, Bruestle J, Jonnal RS, Gao W, et al. Imaging retinal capillaries using ultrahigh-resolution optical coherence tomography and adaptive optics. *Invest Ophthalmol Vis Sci* 2011; 52: 6292–9.
- White VA, Lewallen S, Beare N, Kayira K, Carr RA, Taylor TE. Correlation of retinal haemorrhages with brain haemorrhages in children dying of cerebral malaria in Malawi. *Trans R Soc Trop Med Hyg* 2001; 95: 618–21.
- White VA, Lewallen S, Beare NAV, Molyneux ME, Taylor TE. Retinal pathology of pediatric cerebral malaria in Malawi. *PLoS One* 2009; 4: e4317.
- WHO. Severe falciparum malaria. *Trans R Soc Trop Med Hyg* 2000; 94: S1.
- WHO. Guidelines for the treatment of malaria. 2nd ed. World Health Organization; 2010. <http://www.who.int/malaria/publications/atoz/9789241547925/en/index.html> [29 May 2013 date last accessed].
- WHO. World Malaria Report. 2012, http://www.who.int/malaria/publications/world_malaria_report_2012/report/en/ [29 May 2013 date last accessed].
- Widjaja E, Griffiths PD. Intracranial MR venography in children: normal anatomy and variations. *AJNR Am J Neuroradiol* 2004; 25: 1557–62.
- Williamson TH, Harris A. Ocular blood flow measurement [Review]. *Br J Ophthalmol* 1994; 78: 939–45.

- Wintermark M, Lepori D, Cotting J, Roulet E, Van Melle G, Meuli R, et al. Brain perfusion in children: evolution with age assessed by quantitative perfusion computed tomography. *Pediatrics* 2004; 113: 1642–52.
- Wolfram-Gabel R, Maillot C. Vascular networks of the nucleus lentiformis. *Surg Radiol Anat* 1994; 16: 373–77.
- Wong-Riley M. Energy metabolism of the visual system. *Eye Brain* 2010; 2: 99–116.
- Xu H, Manivannan A, Goatman KA, Jiang HR, Liversidge J, Sharp PF, et al. Reduction in shear stress, activation of the endothelium, and leukocyte priming are all required for leukocyte passage across the blood-retina barrier. *J Leukoc Biol* 2003; 75: 224–32.
- Yadav P, Sharma R, Kumar S, Kumar U. Magnetic resonance features of cerebral malaria. *Acta Radiol* 2008; 49: 566–9.
- Yu DY, Cringle S J. Oxygen distribution and consumption within the retina in vascularised and avascular retinas and in animal models of retinal disease [Review]. *Prog Retin Eye Res* 2001; 20: 175–208.
- Yu PK, Balaratnasingam C, Cringle Stephen J, McAllister IL, Provis J, Yu DY. Microstructure and network organization of the microvasculature in the human macula. *Invest Ophthalmol Vis Sci* 2010; 51: 6735–43.
- Zehetner C, Bechrakis NE. White centered retinal hemorrhages in vitamin b(12) deficiency anemia. *Case Rep Ophthalmol* 2011; 2: 140–4.